2009-01-01

Cis-acting Signals for Replication of Nodamura Virus RNA1

John Joseph Rosskopf
University of Texas at El Paso, jjrosskopf@miners.utep.edu

CIS-ACTING SIGNALS FOR REPLICATION OF *NODAMURA VIRUS* RNA1

JOHN J. ROSSKOPF

Department of Biological Sciences

APPROVED:

_____

Kyle L. Johnson, Ph.D., Chair

_____

Igor Almeida, Ph.D.

_____

Kristine M. Garza, Ph.D.

_____

Kathryn A. Hanley, Ph.D.

_____

Germán Rosas-Acosta, Ph.D.

_____

Patricia D. Witherspoon, Ph.D.

Dean of the Graduate School

CIS-ACTING SIGNALS FOR REPLICATION OF *NODAMURA VIRUS* RNA1

By

JOHN J. ROSSKOPF, B.S.

THESIS

Presented to the Faculty of the Graduate School of

The University of Texas at El Paso

in Partial Fulfillment

of the Requirements

for the Degree of

MASTER OF SCIENCE

Department of Biological Sciences

THE UNIVERSITY OF TEXAS AT EL PASO

December 2009

ACKNOWLEDGEMENTS

I would like to express my gratitude to the many people who have helped my along my way in my graduate studies. Dr. Kyle Johnson, thank you for allowing me to work with you for these years and for being not only my mentor and my boss, but my friend as well. To my committee: Doctors Igor Almeida, Kristine Garza, Katheryn Hanley, and German Rosas-Acosta, I thank you for your assistance and for taking time out of your extremely busy schedules to help me finish my M.S. in Biology.

I would also like to thank all the former and current members, especially Vince Gant, John Upton, and Laura Torres, of the Kyle Johnson lab for their willingness to listen; and for putting up with a slightly rowdy graduate student. Finally, I would like thank my wife Monica and our three children for all of their love, understanding, and support.

ABSTRACT

The family *Nodaviridae* is comprised of two genera: the alphanodaviruses that infect insects and the betanodaviruses, that have been isolated only from fish. *Nodamura virus* (NoV), the type species of the alphanodavirus genus, can lethally infect both insects (mosquitoes, honey bees, and wax moth larvae) and mammals (suckling mice and suckling hamsters). In addition, nodavirus RNAs can replicate in a wide variety of host cells, including those of mammalian, insect, plant, and yeast origin, when introduced by transfection. The nodavirus positive strand RNA genome is segregated into two segments. RNA1 encodes the viral RNA-dependent RNA polymerase (RdRp) that replicates both genome segments via negative strand intermediates, while RNA2 encodes the precursor to the viral capsid proteins. During RNA replication a subgenomic RNA3 is synthesized from RNA1 and is identical to the last 470nt of RNA1. RNA3 encodes proteins B1 and B2 from overlapping reading frames. Protein B1 has no known function and B2 has been shown to suppress RNA interference. In addition, RNA3 has been shown to be required for RNA2 replication.

As a part of ongoing studies to investigate the mechanism of nodavirus RNA replication, we wished to identify *cis*-acting RNA elements (structures or sequences within the RNA) that are required for replication of RNA1. We examined the 3' untranslated region (UTR) of NoV RNA1 for these elements based on the facts that viral UTR's have been shown to be important for viral RNA replication, previous work with *Flock House virus* (FHV) has shown that the replication signals for both FHV RNA1 and RNA1 lie in their 3'UTRs, and that a stem-loop in the NoV RNA2 3'UTR was shown to be essential for its replication. We used three different computer programs running on

the RNAVLab platform to predict the RNA secondary structure of the 3'UTR of NoV RNA1. All three programs consistently predicted the presence of a stem-loop structure (N1-3'SL) near the 3' end of RNA1 (nt 3162-3177).

To test the relevance of the structure in RNA1 replication, we used a well-characterized reverse genetic system for the launch of NoV RNA replication in transformed yeast cells to test the effect of deleting the predicted N1-3'SL structure. Our results showed that the deletion of the stem-loop reduced the accumulation of both positive and negative sense RNA1 and RNA3 replication products in yeast. To determine whether the loop portion, instead of the entire structure, of the N1-3'SL comprised the replication signal for RNA1, we mutated nucleotides in the loop region of N1-3'SL. When we tested this mutant in the yeast cell system, it displayed a severe reduction in RNA1 replication and RNA3 synthesis. The observation that both positive and negative strands were affected suggested that the primary defect was in negative strand synthesis and that the reduction in positive strands was secondary to this defect.

We wondered whether there were also internal *cis*-acting replication signals in NoV RNA1. To facilitate the study of RNA1 template properties without affecting the viral RdRp ORF, we separated the mRNA and template functions of RNA1 onto two different molecules: an mRNA that expresses RdRp but cannot itself be replicated and an RNA1 template that doesn't produce RdRp but can be replicated *in trans* by the expressed RdRp. Four RdRp mRNA constructs have displayed endogenous RNA replication template activity, making it impossible to assess replication of our RNA1 templates. An alternative strategy will be required to produce the RdRp mRNA.

TABLE OF CONTENTS

LIST OF FIGURES

CHAPTER 1

INTRODUCTION

RNA secondary structures present in viral genomes play a role in a variety of processes in the viral life cycle. These structures are often found in the untranslated regions (UTR's) of viral RNA and play roles in viral RNA replication, translation, and protection from nucleolytic digestion (10). The focus of our laboratory is the mechanism of RNA replication in viruses comprising the virus family *Nodaviridae*. These are small viruses that contain bipartite positive sense RNA genomes. These viruses have been used as a model to study mechanisms of RNA replication, viral assembly, and virus structure. The studies detailed here investigate the RNA sequence requirements for replication of the RNA1 genome segment of *Nodamura virus* (NoV), the type species of the alphanodavirus genus of the *Nodaviridae*.

1.1. Nodaviruses

The *Nodaviridae* is a family of icosahedral, non-enveloped viruses with small positive sense RNA genomes that are naturally bipartite. This virus family consists of two genera: alphanodaviruses and betanodaviruses. Members of the alphanodavirus genus primarily infect insects and include NoV, *Black beetle virus* (BBV), *Boolarra virus* (BoV), *Flock House virus* (FHV), and *Pariacoto virus* (PaV). Betanodaviruses infect fish and include *Barfin flounder nervous necrosis virus* (BFNNV), *Greasy grouper nervous necrosis virus* (GGNNV), *Redspotted grouper nervous necrosis virus* (RGNNV), *Striped jack nervous necrosis virus* (SJNNV), and *Tiger puffer nervous necrosis virus* (TPNNV).

NoV was initially isolated from a pool of *Culex tritaeniorhyncus* mosquitoes in Japan in 1956 and has also been shown to lethally infect adult honey bees (*Apis mellifera*), larvae of the Greater wax moth (*Galleria mellonella*), and several species of mosquitoes including *Culex tarsalis*, *Toxorrhynchitis amboinensis*, *Aedes aegypti*, and *Aedes albopictus* (5, 27, 53). An interesting aspect of the nodaviruses is that they have the ability to replicate in a number of different cell types outside of those they naturally infect. In addition, NoV can lethally infect suckling mice and suckling hamsters and neutralizing antibodies against NoV have been isolated from pigs and herons (53, 54).In addition to being able to infect insect cells, FHV and NoV have been shown to be able to replicate their genomes upon transfection into insect cells, plant cells, mammalian cells (6, 7, 28, 55), and the budding yeast *Saccharomyces cerevisiae* (46, 48).

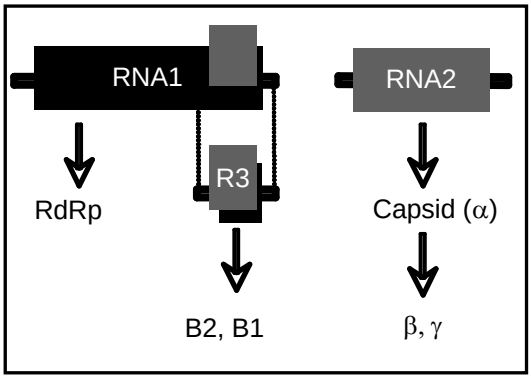

Figure 1. Schematic of nodavirus genome organization. The bipartite NoV genome consists of RNA1 and RNA2. RNA1 encodes the RdRp and RNA2 encodes the capsid precursor protein, which is ultimately cleaved to yield the proteins, β and γ, found in the mature, infectious virion. During RNA replication, a subgenomic RNA3 that is co-terminal with RNA1 is generated; RNA3 encodes proteins B1 and B2.

As shown in 1, the nodavirus positive-strand RNA genome is naturally bipartite. Genomic RNA1 and RNA2 total about 4.5 kb in length. RNA1 encodes the RNA-dependent RNA polymerase (RdRp) that replicates both genomic segments. RNA2

encodes the capsid precursor protein, that upon assembly of progeny RNA, undergoes a maturation cleavage that generates the mature capsid proteins β and γ. In addition a subgenomic RNA3 is generated during RNA replication. RNA3 encodes two nonstructural proteins, B1 and B2, from overlapping reading frames (28). The function of protein B1 is unknown, while protein B2 suppresses RNA interference (RNAi). This ability was first shown for FHV B2 in plants and cultured *Drosophila* cells (34). The FHV and NoV B2 proteins bind short interfering RNAs (siRNAs) and long double strand RNA (dsRNA). NoV B2 suppresses RNAi in insect, mammalian, and human cells (13, 36, 37, 56). NoV B2 has two isoforms, of 134 and 137 aa respectively (27). The B2 proteins of the betanodaviruses SJNNV and GGNNV also act as suppressers of RNAi, although they share little homology with the B2 proteins of NoV and FHV (17, 23). The presence of B2 is also important in maintaining RNA levels for FHV and NoV in cultured cells when compared to deletion mutants that do not encode protein B2. This suggests that RNA replication for these viruses may depend in part on circumventing host RNAi responses (25, 28).

Their small size, relative genetic simplicity, and ability to replicate their genomes in a wide variety of cell types have made nodaviruses attractive candidates for studying the RNA replication mechanisms used by positive strand RNA viruses and for the development of RNA expression systems. The selection of NoV as an RNA replication research model was based on these criteria.

1.2. Nodavirus reverse genetics

A reverse genetic system relies on the use of a cDNA copy of the viral genomic RNAs, enabling researchers to make mutagenic changes to it at the DNA level. Several different versions of this system have used a variety of means to deliver replicable RNA transcripts into the cytoplasm of the host cell, where they can initiate a complete replicative cycle. Pioneered for expression of FHV RNAs, the first such system used a *Vaccinia virus* (VV) recombinant that expressed bacteriophage T7 RNA polymerase to catalyze synthesis of primary transcripts from an FHV RNA expression plasmid. This expression plasmid contained a T7 promoter to direct primary transcription by T7 RNA polymerase, a cDNA copy of RNA1 or RNA2, a *satellite tobacco ringspot virus* self-cleaving ribozyme to generate precise 3' termini, and a T7 terminator to stop transcription. The positioning of the promoter and ribozyme were crucial because the addition or subtraction of even a few nucleotides at the transcript termini severely affected recognition by the RdRp (6).

Cells were first infected with the VVT7 recombinant and then transfected with the FHV RNA expression construct(s). Using this system, DNA-generated transcripts of FHV RNA1 and RNA2 were translated into viral proteins, including the viral RdRp, which replicated the viral RNAs via negative strand intermediates. A similar system was developed in which FHV RNA1 was expressed from a recombinant VV-FHV1 virus, providing both RdRp and a replication template in infected cells (8). However, reliance on these systems imposed a limit of useful information because the co-infection of cells with two different viruses made it hard to decipher which effects could be attributed to which particular virus.

To alleviate this potential limitation, FHV RNA replication systems were developed that used cellular RNA polymerase II to launch replicable FHV transcripts in mammalian cells (25, 26) and in yeast (45, 47, 48). This system, shown schematically for NoV in Figure 3, allows expression of RNA transcripts able to launch nodavirus RNA replication in eukaryotic cells without the potential effects of using a VV recombinant. One problem discovered in using RNA *pol II* systems in mammalian cells was that there was a significant time lag in the detection of RNA replication products (26). Presumably this was due to the fact that the expression plasmids needed to gain entrance to the nucleus, where they are transcribed by cellular RNA *pol II*, and these transcripts needed to be exported to the cytoplasm to begin RNA replication. This problem could be alleviated by transfecting T7 promoter-directed FHV transcription plasmids into a sub-line of BHK-21 cells (BSR-T7/5) that constitutively expressed T7 RNA polymerase in the cytoplasm (11), effectively bypassing the need to transport plasmids and transcripts into or out of the nucleus (3). This system was also used to efficiently launch the replicative cycles of NoV and PaV (27, 29).

1.3. Nodavirus RNA replication

RNA replication is the process of amplification of viral genomic RNA. The RNA replication mechanisms utilized by different families of RNA viruses vary. For viruses with positive strand RNA genomes, RNA replication involves the synthesis of negative strand intermediates that are used as templates to generate further genomic positive

strands. Using FHV as a model, introduction of FHV RNA1 and RNA2 into insect, plant, mammalian, or yeast cells results in initiation of a complete viral replication cycle, as described above and shown schematically in Figure 2 (6, 46, 48, 55).

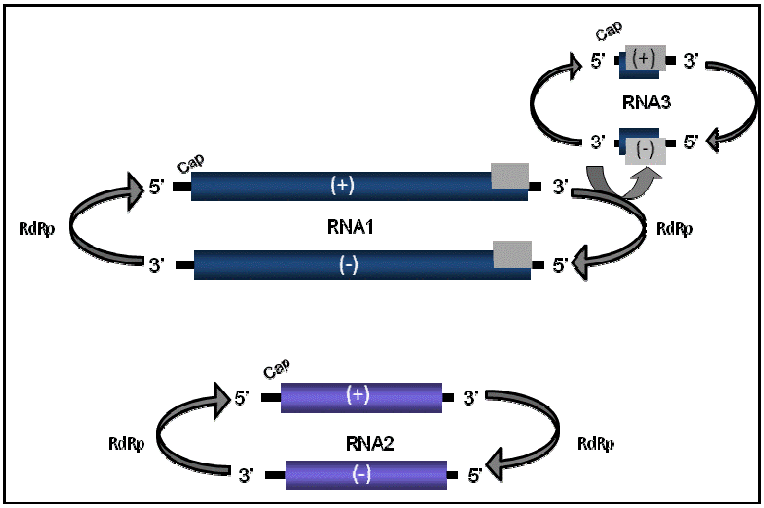

Figure 2. Nodavirus RNA replication. Upon introduction into the cytoplasm, host translation machinery translates the viral RdRp encoded by RNA1. The RdRp synthesizes complementary negative sense transcripts of the genome segments RNA1 and RNA2, which are used as templates for the synthesis of further positive sense RNAs. Subgenomic RNA3 is generated from RNA1 during RNA replication and is also amplified via negative strand intermediates.

Cellular host translation machinery translates RNA1 to yield the viral RdRp. The RdRp recognizes RNA1, presumably by interacting with an as-yet unidentified negative strand promoter, and synthesizes a complementary negative strand from the positive strand template. These negative strands represent only 1-5% of the amount of positive strands produced during RNA replication and are used as templates for further positive strand synthesis, a pattern that is a hallmark of positive strand RNA viruses (3, 44).

During RNA1 replication, subgenomic RNA3 is synthesized and replicated in a similar fashion. Although the precise mechanism by which RNA3 is synthesized is unclear, two possible mechanisms have been proposed (62). The first mechanism

involves premature termination by the RdRp during negative strand RNA1 synthesis, producing negative sense RNA3 molecules that are copied into positive strands, and subsequently replicated, by the RdRp. The second mechanism proposes internal initiation on a putative internal promoter site in a negative sense RNA1 template, allowing the viral RdRp to synthesize positive sense RNA3. This second model does not account for the production of negative strand copies of RNA3.

For FHV, the synthesis of RNA3 is dependent on a long distance base pairing interaction within the positive strand of RNA1 that produce an RNA secondary structure near the putative subgenomic RNA3 start site. This structure may serve in the positive sense as a termination signal to produce negative strand RNA3 or in the negative sense as a promoter for synthesis of positive strand RNA3. The observations that negative strand copies of RNA3 can be detected in cells transfected with FHV RNA1, that the negative strand of RNA3 can be used as a template for positive strand RNA3 synthesis, and that RNA3 replicates via negative strand intermediates (16, 35), lend support to the premature termination model. However, additional experimentation will be required to determine the exact mechanism of RNA3 synthesis.

The synthesis of FHV RNA2 and RNA3 appears to be counter-regulatory (62). At early times in FHV RNA replication, RNA3 (and RNA1) accumulate, while RNA2 is difficult to detect. When RNA2 synthesis increases, the levels of RNA3 (and RNA1) decrease, suggesting that RNA2 replication inhibits RNA3 synthesis (62). In contrast, RNA2 is unable to replicate in the absence of RNA3 replication (16). This counter-regulatory mechanism, in which RNA2 replication is dependent on RNA3 and RNA1 levels are affected by the presence of RNA2, has been postulated as a way to ensure

that only one copy of RNA1 and one copy of RNA2 is packaged into the progeny virion. A similar regulatory mechanism has been proposed for NoV, in light of the observation that a single U-to-C change in NoV RNA3 results in a 70% reduction in RNA2 synthesis (27).

During RNA replication, dimeric negative-sense RNAs are synthesized for both FHV and NoV (3, 27). For FHV, these transcripts consist of head-to-tail homodimers of RNA1, RNA2, and RNA3, and of heterodimers of RNA2 and RNA3 in two different orientations: RNA2/3 and RNA3/2 (3). Similar dimeric molecules are also detected for NoV (27). The exact role of these dimers has not been established, but the ability of the FHV RdRp to resolve these dimers into monomeric RNA isoforms during positive strand synthesis suggests that these dimeric molecules may serve as replication intermediates (3). Further work by Albariño *et al.* (2003) showed that, for FHV, the resolution of monomers of RNA from dimeric forms is directed by discrete regions in the 3' termini of the viral RNAs, specifically the 3' 50nt of FHV RNA2 and the 3' 108nt of FHV RNA1 (2). The ability to generate these monomers suggests that the RdRp can either initiate or terminate RNA replication from their putative signals when internally located within a larger molecule (3), lending weight to the idea that these dimers may play a role in nodavirus RNA replication.

Nodavirus RNA1 serves as both a template for RNA replication and as an mRNA for translation of the viral RdRp. This means that changes made to RNA1 can affect the function of the RdRp as well as the ability of the RNA to serve as a replication template. In order determine which *cis*-acting sequences in RNA1 influence its replication without introducing changes into the RdRp, these two functions of FHV RNA1 were separated

onto two separate RNA molecules. The ability of the RdRp to replicate an exogenous template was tested in yeast and mammalian cells (16, 35, 47). This *trans* system of replication is based on expression of 1) an FHV RdRp mRNA that cannot recognize its own RNA template and 2) a template RNA that does not encode the RdRp. To facilitate further RNA replication studies, we are in the process of creating a similar system for examination of NoV RNA replication in yeast cells, as described in section 3.2.

Nodavirus RNA replication localizes to mitochondria in infected or transfected cells. Microscopic analysis of thin sections of muscle tissue from NoV-infected *Galleria mellonella* larvae and suckling mice showed marked morphological changes in the mitochondria of infected muscle cells. At late stages of infection, assembly of virions takes place around the mitochondria and arrays of virions are seen in membrane-associated vesicles (18, 19). In FHV infected *Drosophila* DL-1 cells, the RdRp is tightly membrane associated and localizes to the membrane fraction in cell extracts subjected to gradient centrifugation. Immunofluoresence analysis and electron microscopy was used to show that FHV RNA replication takes place in membrane-bound spherules that form between the outer and inner mitochondrial membranes (39). Electron microscopic tomography was used to show that these spherules were invaginations in the outer mitochondrial membrane of about 50nm in size, with an opening to the cytoplasm of about 10nm (32). Miller *et al.* (2002) showed that the signal targeting FHV protein A to the mitochondria is contained in the amino terminal 46aa of protein A, corresponding to nt 1-138 of FHV RNA1 (38). When this signal was replaced with an endoplasmic reticulum (ER) targeting signal, protein A was re-targeted to ER membranes and replication of FHV RNA1 was 2-13 fold higher than that seen for wild type RNA1 (40).

The ability to continue FHV RNA1 replication, even on membranes from a different organelle, was shown to be due to recruitment of viral RNA from the cytoplasm to the membrane-bound RdRp by a region in FHV protein A (amino acids 36-370) that interacts with two stem-loops (nt 68-205) in FHV RNA1 (58).

Perhaps it is not surprising, in light of the localization of the RdRp to membranous structures in infected cells, to discover that membranes are essential for the protein A polymerase activity. This was shown originally for BBV. During attempts to purify the BBV RdRp activity to homogeneity, it was discovered that treatment of replicase fractions with detergent inactivates replicase enzymatic activity (21). For FHV, cell-free extracts from infected *Drosophila* cells were shown to synthesize RNA replication products *in vitro*. However, the use of detergents to solubilize membranes disrupted the ability of the RdRp to synthesize new positive RNA strands, while its ability to synthesize negative strands was maintained (60). Restoration of complete RNA replication *in vitro* was accomplished by the addition of exogenous glycerophospholipid (60). Replication of positive strand RNA from negative strand templates depends on the presence of neutral or negatively charged glycerophospholipids, while the head group or acyl chain alone was not sufficient for positive strand synthesis to occur (60). The dependence of RdRp activity on glycerophospholipids, its sensitivity to detergents, and its association with mitochondria suggest that the RdRp requires some component of membranes in order to function properly.

1.4. Nodavirus RNA replication in yeast

FHV was the first animal virus shown to replicate its genome in the yeast *Saccharomyces cerevisiae* and, until recently, the only virus able to reproduce its entire life cycle in yeast, including the synthesis of infectious progeny virus (48). NoV has also been shown to be able to fully replicate its genome and to make progeny virions in yeast (46). A number of viruses, including human papillomavirus (HPV), *Brome mosaic virus*, *Tomato bushy stunt virus, Indian mung bean yellow mosaic virus, and Bovine papilloma virus-1*, can partially replicate their genomes in yeast (4, 24, 42, 49, 61).

To facilitate the study of nodavirus RNA replication in yeast, a system was developed using yeast shuttle vectors that are able to propagate in two different host species (in this case yeast and *E. coli*). This system was originally developed for FHV and consisted of a plasmid that directed transcription of FHV RNA1 (pF1) and another, FHV RNA2 (pF2). Plasmids pF1 and pF2 contained an inducible yeast *GAL1* promoter, the cDNA of FHV RNA1 or RNA2 genomic RNAs, a *hepatitis delta virus* (HDV) ribozyme, and, for the RNA2 plasmid, a yeast *ADH* terminator. Plasmids pF1 and pF2 are derived from the parental yeast shuttle vectors YEplac112 and YEp351, respectively. A similar system was later developed for NoV (46). The plasmids TpG-N1 and LpG-N2 were constructed; these plasmids contained the NoV RNA1 and RNA2 cDNAs in place of their FHV counterparts in pF1 and pF2 (46). With these systems the ability of both FHV and NoV to fully replicate their genomes was established. Interestingly, accumulation of NoV RNA2 was much less in yeast as compared to that of FHV RNA2, for reasons that remain unclear (46).

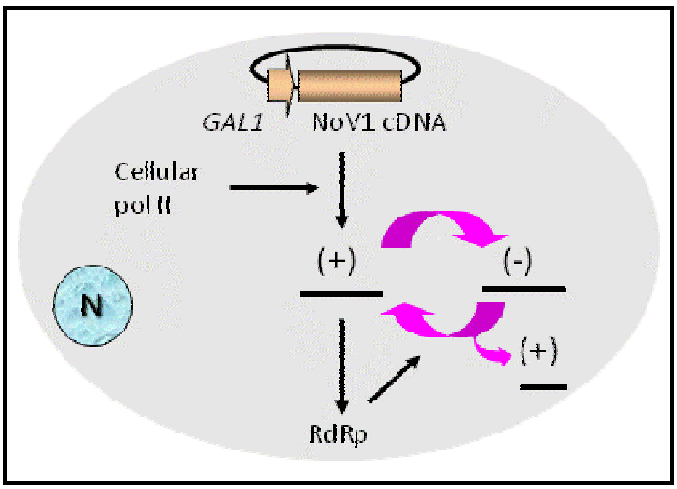

Figure 3. Induction of primary transcription in plasmid-transformed yeast cells. Primary transcription from the inducible yeast *GAL1* promoter is catalyzed by cellular RNA polymerase II. Transcription is induced by growing the cells in medium containing galactose. A complete viral replicative cycle is initiated by the resulting primary transcripts.

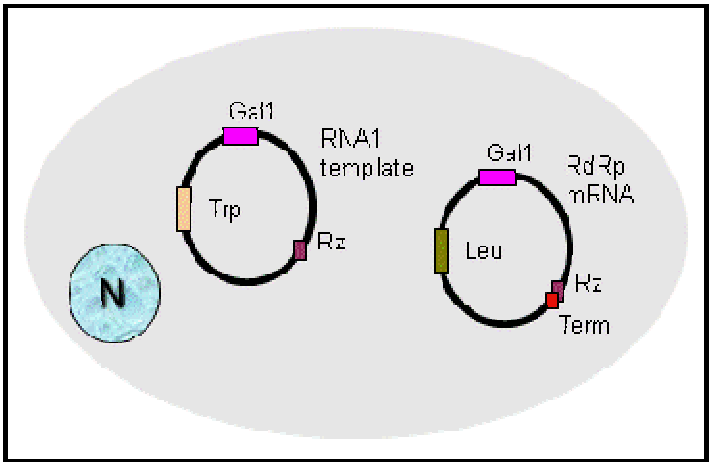

Figure 4. Plasmid transformation of yeast cells. Transformations involve cells of the *Saccharomyces cerevisiae* synthetic deletion BY4733 *(*genotype *MATa his3Δ200 leu2Δ0 met15Δ0 trp1Δ63 ura3Δ0),* which is unable to synthesize essential nutrients histidine (his), leucine (leu), methionine (met), tryptophan (trp), and uracil (ura). The defects in histidine, methionine, and uracil biosynthesis are complemented by the addition of these nutrients to the medium. The defects in tryptophan and leucine biosynthesis are complemented by transformation of the cells with plasmids that express the *TRP1* and *LEU2* yeast selectable markers. This allows nutritional selection for cells that have taken up both plasmids. Cells that lack one or both of these markers will not form colonies on selective medium.

The parental plasmid YEplac112 (20) contains a yeast *TRP1* selectable marker, while the parental plasmid YEp351 (22) contains a *LEU2* selectable marker. These genes allow for nutritional selection of transformed yeast cells. The *S. cerevisiae* yeast strain used in these studies, BY4733, is a synthetic deletion strain that contains mutations in genes required to synthesize the essential nutrients methionine, uracil, histidine, tryptophan, and leucine (9). Methionine, uracil, and histidine are added to the medium, whereas the defects in tryptophan and leucine synthesis can be complemented by transforming the cells with plasmids YEplac112 (or derivatives pF1 or TpG-N1) and YEp351 (or derivatives pF2 or LpG-N2), as shown schematically in Figure 4. Competent yeast cells are transformed with these plasmids and, upon induction with galactose, the yeast *GAL1* promoter is used by cellular RNA polymerase II to direct synthesis of NoV (or FHV) primary transcripts. These transcripts are translated into proteins by the host cellular machinery. Once the RdRp is synthesized, it can replicate the primary transcripts, producing RNA1, RNA2 and subgenomic RNA3. Using this system, we are able to fully recapitulate the viral RNA replication cycle (46), which allows us to study the replication of NoV in single-celled eukaryotic organisms under well-defined conditions.

1.5. NoV RNA secondary structures and RNA replication

The underlying RNA *cis*-acting elements, i.e. intrinsic sequences or structures in the RNA that influence NoV RNA replication, are mostly unknown. However, specific RNA secondary structures are reasonable candidates for influencing NoV RNA1 replication. RNA secondary structures have been shown to be important for the life

cycles of many viruses. These structures are commonly found in the untranslated regions of viral RNA and play roles in promoting viral RNA replication, initiating translation, and protecting viral RNAs from nucleolytic digestion (10). For FHV, secondary structure plays a role in the synthesis of the subgenomic RNA3. Lindenbach *et al.* (2002) demonstrated that the generation of the subgenomic RNA3 was dependent on long range base pairing reactions within FHV RNA1 and that the structure formed by this base pairing was more important than the sequence of the complementary regions (35). A similar long-range interaction in the RNA1 of NoV was also hypothesized to be necessary for the synthesis of NoV RNA3. In NoV RNA1, a U-to-C mutation at position 1274, 1458 nucleotides upstream of the NoV RNA3 start site, results in an 80% reduction in NoV RNA3 synthesis and a corresponding 70% reduction in the replication of RNA2 (27). The effect of this mutation on NoV RNA3 synthesis despite its distance from the NoV RNA3 start site, and our ability to predict long distance base pairing in NoV RNA3 analogous to that seen for FHV (K.L. Johnson, personal communication), suggests that RNA secondary structures play a key role in the synthesis of nodavirus RNA3.

For NoV, the role of RNA secondary structures in RNA replication has been described in detail only for RNA2. Using computer prediction of RNA secondary structure based on free energy, a stem loop was predicted to form in the 3' UTR of NoV RNA2 (nt 1299-1322) (57) and the existence of this predicted stem loop was verified by nuclease mapping (Rosskopf, Upton, and Johnson, manuscript in preparation). The predicted structure was deleted from the NoV RNA1 cDNA clone and the effect of the deletion was tested in transformed yeast cells, using the reverse genetic system

developed for NoV in yeast, described in section 1.4. Upon deletion of this stem loop, NoV RNA2 negative strand synthesis was shown by Northern blot hybridization to be severely inhibited. Further studies revealed a corresponding decrease in synthesis of positive strand RNA2. Since these positive strands are synthesized from negative strand intermediates this defect is considered secondary to the negative strand defect. Since deletion of the stem loop from RNA2 leads to abrogation of negative strand synthesis, we believe that the structure constitutes an essential element of the RNA2 negative strand promoter. Moreover we have shown that a 3' terminal stem loop structure is conserved among the RNA2s of BBV, BoV, FHV, NoV, PaV, GGNNV, and SJNNV (57), although the role of the stem loop in replication of these RNA2 species remains to be determined. However, since the predicted stem loop occurs within the 3'-terminal 50 nt of FHV RNA2, a region that Albariño *et al.* (2003) showed was essential for its replication, it is likely that the analogous structural element is involved in FHV RNA2 replication as well (2).

1.6. NoV and cellular host factors.

Viruses do not encode all of the factors needed for successful completion of their life cycle, so host cellular factors play a wide range of roles in the life cycle of viruses. These host cellular factors are diverse, including proteins as well as nucleic acids, and contribute to the life cycles of viruses in different ways, depending on the virus. For positive strand RNA viruses, host factors play important roles in selection and recruitment of RNA templates in addition to replicase assembly (1).

For nodaviruses, relatively little is known about which host factors are required for RNA replication. For FHV, the heat shock protein chaperones HSP90 and HSP70 play a role in this process. In FHV infected *Drosophila* S2 cells, inhibition of HSP90 by geldanamycin results in reduced accumulation of FHV viral RNA, protein A, and virions (31). Little inhibition was noted when pre-formed replication complexes were used, suggesting that HSP90 might influence replicase assembly (31). Further studies showed that the inhibition of FHV protein A synthesis was not due to proteasomal inhibition, protein degradation, changes in the UTRs, or intracellular location (12). However, these results do not hold true across cell types. HSP90 knockouts in *S. cerevisiae* have little effect on FHV RNA replication, but yeast knockouts in the HSP70 co-chaperone *YDJ1* show significant reduction in FHV RNA replication (59). Although the host cellular factor requirement may be different among cell types for FHV RNA replication, the fact that the protein chaperone pathways are involved in both cell types suggests that this pathway is important for FHV RNA replication.

1.7 Summary

The studies described here take two approaches to identify *cis*-acting elements in NoV RNA1 that are important for RNA replication: 1) targeting a predicted RNA structure element near the 3' end of RNA1 and 2) performing a deletion analysis to define the minimal sequence requirements for RNA1 replication. In the first approach, we used computer prediction software to show that a stem-loop structure was predicted to form in the 3' UTR of NoV RNA1. **We hypothesized that the predicted structure was essential for RNA1 replication.** To test this hypothesis, we utilized site-directed

mutagenesis to ascertain the contribution of this structure to the viral replicative cycle. We compared a deletion mutation that removed the predicted structure entirely to one in which only the loop region of the structure was altered. During the course of these studies, it became clear that the RNA1 loop contained a sequence identical to one found in a stem-loop structure near the 3' end of NoV RNA2. Therefore, we also tested the effect on RNA replication of mutating the loop sequence in RNA2.

In the second approach, we attempted to map the minimal *cis*-acting RNA elements in RNA1 required for its replication. This necessitated our creation of a *trans* system for RNA1, so that we could separate the two functions of RNA1, i.e., a template for RNA replication and an mRNA for RdRp synthesis, onto two different RNA molecules. Using this system, we could study the effect of mutating the RNA1 template without affecting synthesis of the RdRp. We therefore constructed a panel of five deletion mutants that retained varying regions of RNA1 sequence, which we planned to test for their ability serve as templates for RNA replication. We also constructed four different versions of an RdRp mRNA in an attempt to generate an RdRp that would not replicate its own template.

Together these lines of research will contribute to our understanding of RNA replication in NoV, and possibly other virus systems. This knowledge could assist us in the development of NoV-based vectors for vaccine development or gene expression, both of which are goals of our laboratory.

CHAPTER 2

MATERIALS AND METHODS

2.1. Cells and growth conditions

Plasmids were propagated in different *Escherichia coli* strains, as follows. PCR products subcloned into the pGEM-T Easy® (Promega) TA vector were transformed into the JM109 strain (Promega). The remaining plasmids were transformed into the NEB-10β strain (New England Biolabs). Transformed cells were grown on Luria-Bertani (LB) agar plates or in LB broth, supplemented in each case with ampicillin.

RNA replication studies were carried out in the yeast *Sacharromyces cerevisiae* using synthetic deletion strain BY4733 *(*genotype *MATa his3Δ200 leu2Δ0 met15Δ0 trp1Δ63 ura3Δ0)* (9). Competent cells were prepared and the cells subsequently transformed with plasmid RNA using the Frozen-EZ Yeast Transformation II™ kit (Zymo Research Corp., Orange, CA). Yeast cells were co-transformed with experimental plasmids containing appropriate selectable markers to allow growth of yeast cells in media selective for *LEU2* and *TRP1.* Selection of leu+trp+ colonies was performed at 30^{o}C on selective solid minimal medium (YNB) plates lacking tryptophan and leucine but supplemented with methionine, uracil, and histidine, and containing glucose as a carbon source, For induction of RNA transcription from the *GAL1* promoter, leu+trp+ colonies were inoculated into selective liquid medium containing 2% galactose and grown for 24 hours at 30^{o}C.

2.2. Plasmids used

Parental plasmids. Plasmid TpG-N1 contains (in a 5'-to-3' direction) an inducible yeast *GAL1* promoter, a cDNA copy of NoV genomic RNA1, a cDNA copy of the hepatitis delta virus (HDV) antigenomic ribozyme, and a yeast *TRP1* selectable marker (46) in a YEplac112 backbone which also contains an *E. coli* origin of replication and an ampicillin resistance gene. Parental plasmid YEplac112 (20) lacks the NoV RNA1 cDNA but contains the *TRP1* selectable markers. These plasmids are shown schematically in Figure 5. The NoV RNA1 portion of TpG-N1 is also shown schematically in Figure 9.

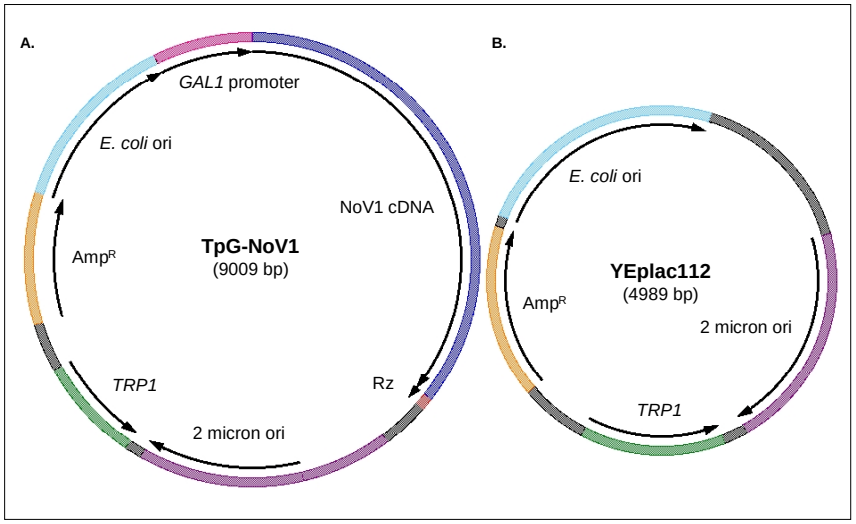

Figure 5. Schematic of plasmids TpG-N1 and YEplac112. Panel A. TpG-Nov1 contains (in a 5' to 3' direction) a yeast *GAL1* promoter, a cDNA copy of NoV RNA1, and an HDV ribozyme cDNA, which have been cloned into the yeast transcription plasmid YEplac112 (**panel B**). The yeast *TRP1* selectable marker allows for selection of yeast cells that have taken up the plasmid.

Plasmid LpG-N2 contains an inducible yeast *GAL1* promoter, a cDNA copy of NoV genomic RNA2, a cDNA copy of the HDV ribozyme, yeast *ADH* polyadenylation and termination signals, and the yeast *LEU2* selectable marker (46) in a YEp351 backbone which contains an *E. coli* origin of replication and an ampicillin resistance

gene. Parental plasmid YEp351 (22) lacks the NoV RNA2 cDNA but contains the *LEU2* selectable marker. These plasmids are shown schematically in Figure 6.

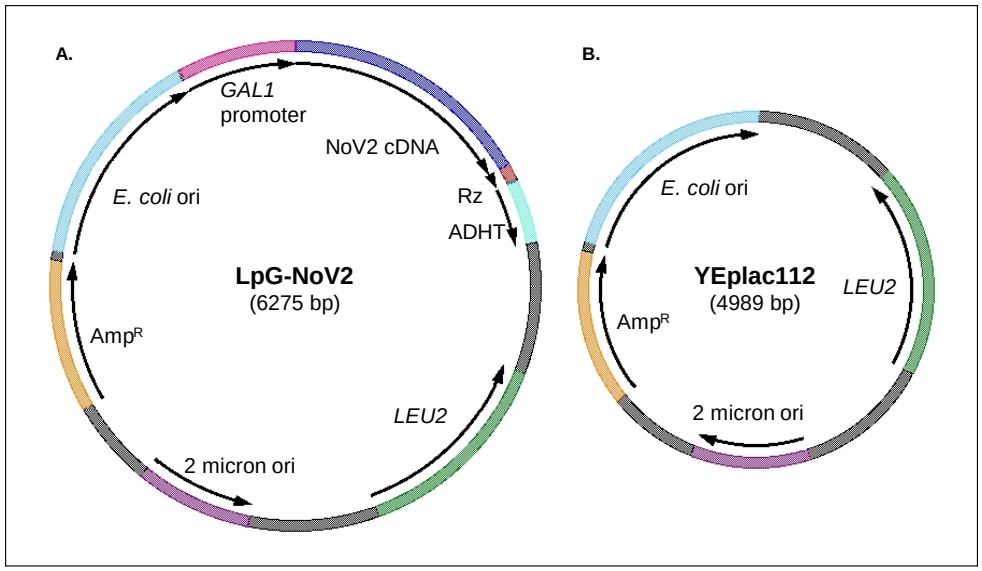

Figure 6. Schematic of plasmids LpG-N2 and YEp351. Panel A. LpG-NoV2 contains (in a 5' to 3' direction) a yeast *GAL1* promoter, a cDNA copy of NoV RNA2, an HDV ribozyme cDNA, and an *ADH* terminator, cloned into the yeast transcription plasmid YEp351 (**panel B).** The yeast *LEU2* selectable marker allows for selection of yeast cells that have taken up the plasmid.

Plasmids pNoV1(0,0) and pNoV2(0,0) contain cDNA copies of NoV RNA1 or RNA2, respectively, flanked by a T7 promoter and the cDNA of the HDV ribozyme; these plasmids contain an *E. coli* origin of replication and an ampicillin resistance gene, as described previously (27). These plasmids are shown schematically in Figure 7.

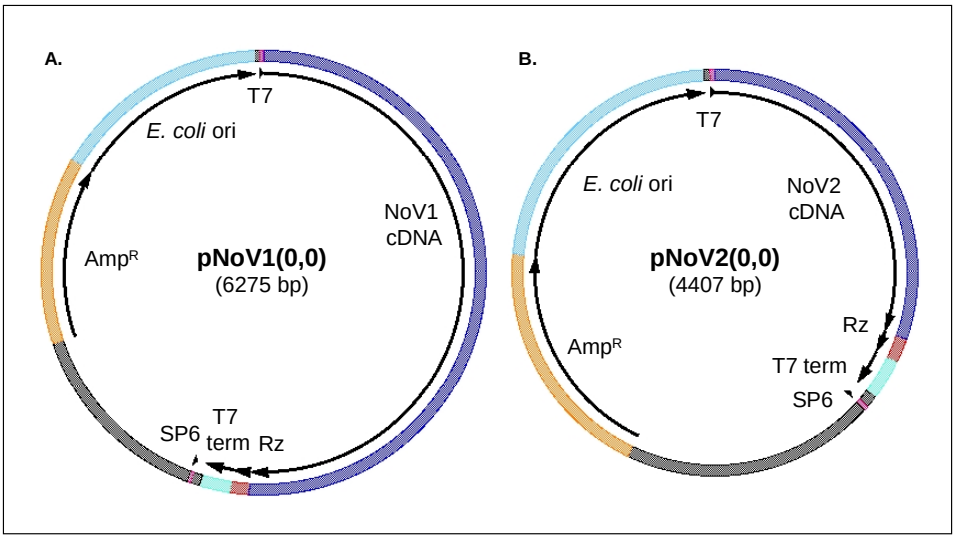

Figure 7. Schematic of plasmids pNoV1(0,0) and pNoV2(0,0). Panel A. Plasmid pNoV1(0,0) contains (in a 5' to 3' direction) a T7 promoter, a cDNA copy of NoV RNA1, an HDV ribozyme cDNA, a T7 terminator, and an SP6 promoter. **Panel B.** pNoV2(0,0) contain (in a 5' to 3' direction) a T7 promoter, a cDNA copy of NoV RNA2, an HDV ribozyme cDNA, a T7 terminator, and an SP6 promoter.

Plasmid pGTE-GFP*BsmBI* is a pGEM-T-Easy derivative that contains the coding region of mammalian codon-optimized green fluorescent protein (GFP). It was constructed by PCR amplification of the GFP ORF from the plasmid pGREENLANTERN (Invitrogen) using primers that placed a unique *BsmBI* site (with a GTAC 5' overhang compatible with an *NcoI* overhang) at the 5' end of the GFP ORF and a unique *MluI* site at its 3' end. The GFP ORF can therefore be liberated as a 719 bp fragment by digestion with *BsmBI* and *MluI*.

Plasmid TpG-N1Δ3'SL. The deletion of the predicted N13'SL stem loop in NoV RNA1, corresponding to nucleotides 3162-3177, was carried out by PCR based circular mutagenesis followed by *DpnI* selection, as described (52). Briefly, plasmid pNoV1(0,0) was amplified using *Pfu-Turbo* DNA Polymerase (Stratagene) and the following mutagenic oligonucleotide primers, which are complementary to one another. The primer sequences are 5'GCGTGGTAAATGAGTGATTCAAACCCGAACTAGGCTTAT-

GCC3’ (identical to nt 3141-3161, followed by nt 3178-3198 of the NoV1 cDNA) and 5’CGCATAAGCCTAGTTCGGGTTTGAATCACTCATTTACCACGC3’ (complementary to nt 3198-3178, followed by nt 3161-3141 of the NoV1 cDNA) The omission of nucleotides 3162-3177 from the primers effectively loop out that sequence during the circular PCR reaction, resulting in deletion of the nucleotides that comprise the predicted RNA1 stem loop. The region of interest was confirmed by sequencing and a small DNA fragment (*BamHI*$_{2848}$-*RsrII*$_{3234}$) containing the desired mutation was isolated and ligated into plasmid TpG-N1 using standard techniques (52). The resulting plasmid, TpG-N1Δ3’SL, contains the entire sequence of TpG-N1 except nt 3162-3177 of the NoV1 cDNA, which form stem loop N13’SL. The NoV RNA1 portion of this plasmid is shown schematically in Figure 9.

Plasmid TpG-N1-lm. We changed the sequence of the loop region in the predicted RNA1 stem loop (nt 3166-3172 of the RNA1 cDNA) from 5’UACCCAUCUC3’ to 5’UA**GGGUAGA**C3’ using circular PCR mutagenesis followed by *DpnI* selection. This was performed as described above, except that we used plasmid pNoV1(0,0) as a template and the mutagenic primers 5’GTAAATGAGTGATTCATCGT**GGGTAGA**GAC-GAAACCCGAACTAGGC3’ (identical to nt 3146-3165, followed by the mutant sequence GGGTAGA, then nt 3173-3172 of the RNA1 cDNA) and 5’GCCTAGTTCGGGTTTCGT-C**TCTACCC**ACGATGAATCACTCATTTAC3’ (complementary to nt 3191-3173 of the RNA1 cDNA, the loop mutations for nt 3172-3166, then nt 3165-3146 of the RNA1 cDNA). The presence of the desired mutations was confirmed by DNA sequencing and a small fragment (*BamHI*$_{2848}$-*RsrII*$_{3234}$) containing the desired mutation was isolated and

ligated into plasmid TpG-N1 using standard techniques, resulting in plasmid TpG-N1-lm. The NoV RNA1 portion of this plasmid is shown schematically in Figure 9.

Plasmid LpG-N2-lm. We changed the sequence of the loop region in the predicted RNA2 stem loop (nt 1308-1314) from 5'UACCCAUCUC3' to 5'UA**GGGUAGA**C3' using circular PCR mutagenesis followed by *DpnI* selection. This was performed as described above, except that we used plasmid pNoV2(0,0) as a template and the mutagenic primers 5'CGTAGCACCGACCCTATA**GGGTAGA**CTAGG-GTCTTCAACC3' (identical to nt 1290-1307, followed by the mutant sequence GGGTAGA, then nt 1315-1329 of the RNA2 cDNA) and 5'GGTTGAAGACCCTAG**TCT-ACCC**TATAGGGGTCGGTGCTACG3' (complementary to RNA2 nucleotides 1329-1315, followed by the mutant loop sequence, and nt 1307-1290). The presence of the desired mutations was confirmed by DNA sequencing and a small fragment (*EagI*$_{924}$-*RsrII*$_{1366}$) containing the desired mutation was isolated and ligated into plasmid LpG-N2 using standard techniques, resulting in plasmid LpG-N2-lm. The NoV RNA2 portion of this plasmid is shown schematically in Figure 11.

Plasmid LpG-RdRp. To produce an RdRp mRNA from which protein A could be translated but which could not itself serve as an RNA replication template, our initial strategy was to delete 3 nt (nt 1-3) from the 5'UTR and the entire 3'UTR (nt 3154-3204) from the RNA1 cDNA clone in plasmid TpG-N1. We used PCR to delete nt 1-3 with plasmid TpG-N1 as a template and primers 5'AACTGCAGCAAGCTTGAATCCAAAAC-TCAAAATG-CTG3' (introduces a *PstI* site and a *HindIII* site, then is identical to nt 4-27 of the NoV RNA1 cDNA) and 5'GGCTGATTTCGTAATGACGAAAACCAGCGGCCCTT-ATGG3' (complementary to nt 430-392 of NoV1). The resulting PCR product was

ligated into the pGEM-T-Easy vector (Promega) to yield subclone pGTE-YEpNA5pr. This subclone was digested with *PstI* and *MluI* and a 365 bp fragment containing NoV1 nt 4-365 was isolated. This fragment was ligated to plasmid TpG-N1 to yield plasmid TpG-N1-5' insert.

We then used PCR to delete nt 3154-3204, with template TpG-N1 and primers 5'GCCAAGCTGGAGCAGCTGGCTCAGGAGACGCAAGCAACGATCC3' (identical to nt 2831-2789 of NoV1) and 5'GGTCGGACCGCGAGGAGGTGGAGATGCCATGCCGAC-CCTCATTTACCACGC3' (complementary to nt 3142-3205, then to nt 3153-3141, with a net deletion of nt 3204-3154). The resulting PCR product was ligated into the pGEM-T-Easy vector (Promega) to yield subclone pGTE-YEpNA3pr. This subclone was digested with *BamHI* and *RsrII* and a 342 bp fragment was isolated. This fragment was ligated into TpG-N1-5'insert to generate plasmid TpGN1-RdRp.

Since we wished to use this plasmid to transform yeast cells together with TpGN1-based RNA replication template plasmids (containing the *TRP1* selectable marker), we elected to construct the RdRp-expressing plasmid in a LpG-N2 (YEp351) backbone containing the *LEU2* selectable marker. We therefore digested TpGN1-RdRp with *PstI* and *RsrII* and ligated the resulting 3180 bp fragment into a LpG-N2 vector cut with the same enzymes. The final plasmid, LpG-RdRp, contains in a 5'-3' direction: an inducible yeast *GAL1* promoter, a cDNA copy of RNA1 that has had the 5'-terminal 3nt and entire 3' UTR deleted, the HDV ribozyme, yeast *ADH* polyadenylation and termination signals (ADHT), and the yeast *LEU2* selectable marker. The portion of this plasmid that contains the RdRp coding region and the ribozyme cDNA is shown schematically in Figures 16 and 18.

Plasmid LpG-RdRpΔRz. To determine whether the RdRp was initiating RNA replication in the RNA secondary structures of the HDV ribozyme, we deleted it from the LpG-RdRp plasmid. This is done by PCR using template TpG-N1 and primers 5'GCCAAGCTGGAGCAGCTGGCTCAGGAGACGCAAGCAACGATCC3' (identical to nt 2789-2831 of NoV1) and 5'GCGGTACCTCATTTACCACGCCCACGCGACCCAGC3' (complementary to nt 3127-3154, then adds a *KpnI* site, followed by a CG dinucleotide). This subclone was cut with *BamHI* and *KpnI* and the appropriate fragment was ligated to *KpnI-BamHI* vector and *KpnI-KpnI* fragments from LpG-RdRp, resulting in the plasmid LpG-RdRpΔRz. This plasmid contains RNA1 nt 4-3154, the 3'UTR (nt 3154-3204 in RNA1) deletion and a deletion of the HDV ribozyme. The portion of this plasmid that contains the RdRp coding region and the ribozyme cDNA is shown schematically in Figure 18.

Plasmid LpG-RdRpΔ20. To determine whether a cryptic *cis*-acting signal might reside near the 3' end of the RdRp coding region, we deleted the C-terminal 20 amino acids of the RdRp. We suspected that these amino acids might be dispensable, since they were not conserved with the RdRp's of five other nodaviruses (29). This was done by PCR using template TpG-N1 and primers 5'GCCAAGCTGGAGCAGCTGGCTCAG-GAGACGCAAGCAACGATCC3' (identical to nt 2789-2831 of NoV1) and 5'GCCGGACCGCGAGGAGGTGGAGATGCCATGCCGACCCTCACTTACTTGGGCCA-CTTGTTGG3' (complementary to nt 3067-3087, adds the complement of a UGA stop codon, and then is complementary to nt 1-29 of the HDV ribozyme). The resulting 339 bp PCR product was subcloned into the pGEM-T-Easy vector (Promega), yielding plasmid pGTE-Δ20. The subclone was cut with *BamHI* and *RsrII* and ligated into LpG-

RdRp cut with the same enzymes, to yield the plasmid LpG-RdRpΔ20. This plasmid contains RNA1 nt 4-3154, the 3'UTR (nt 3154-3204 in RNA1) deletion, and the deletion of the last 20 amino acids (60 nt – nt 3093-3153) of the RdRp. The portion of this plasmid that contains the RdRp coding region and the ribozyme cDNA is shown schematically in Figure 18.

Plasmid LpG-RdRpΔ20ΔRz. To determine whether both the Δ20 deletion and the ΔRz would destroy the endogenous RdRp activity, PCR was used to make the double deletion. This is done by PCR using template TpG-N1 and primers 5'GCCAAGCTGGA-GCAGCTGGCTCAGGAGACGCAAGCAACGATCC3' (identical to nt 2789-2831 of NoV1) and 5'GCGGTACCTCACTTACTTGGGCCACTTGTTGGTGCC-CTGGC3' (complementary to nt 3058-3087, adds the complement of a UGA stop codon, and then adds a *KpnI* site followed by a CG dinucleotide). The resulting 310 bp PCR product was subcloned into the pGEM-T-Easy vector (Promega), yielding plasmid pGTE-Δ20ΔRz. This subclone was cut with *BamHI* and *KpnI* and the appropriate fragment was ligated to *KpnI-BamHI* vector and *KpnI-KpnI* fragments from LpG-RdRp, resulting in the plasmid LpG-RdRpΔ20ΔRz.This plasmid is deleted for nt 1-3 and the entire 3'UTR as well as both the C-terminal 20 aa of the RdRp and the HDV ribozyme. The portion of this plasmid that contains the RdRp coding region and the ribozyme cDNA is shown schematically in Figure 18.

Plasmid TpG-N1-NcoI. In order to facilitate introduction of heterologous genes such as GFP into RNA1, PCR was used to introduce a unique *NcoI* site (CCATGG) at the authentic protein A start codon (nt 19 in TpG-N1). This resulted in three nt changes: A20C, A21C, and C25G. Plasmid TpG-N1 was used as a template, and the

oligonucleotide primers contained the sequences 5’ CGTCTAGACTGCAGTATTGAAT-CCAAAACTCACCATGGTGAACTACG3’ (identical the 3’-terminal terminal 6nt of the *GAL1* promoter, then to nt 1-19 of the RNA1 cDNA, adds the CC dinucleotides in place of nts 20 and 21, identical to nt 22-24, adds a C in place of nt 25, then identical to nt 26-34) and 5’GCGGCCGTTATGG-CAAGGGAAA-TAGTCTCC-3’ (complementary to nt 408-375 of the RNA1 cDNA). The resulting PCR product was subcloned into the pGEM-T-Easy vector (Promega) and the presence of the mutations was confirmed by DNA sequencing. The subclone was digested with *PstI* and *MluI* and a small fragment that contained these mutations was re-ligated into a TpG-N1 vector cut with the same enzymes to generate plasmid TpG-N1-*NcoI*.

Plasmid TpG-N1-GFP. To introduce the GFP coding region into NoV RNA1, plasmid TpG-N1-*NcoI* was digested with RsrII and NcoI to yield a 5795 bp vector fragment and, in a parallel reaction, with MluI and RsrII, to yield a 2875 bp fragment. A 719 bp GFP-containing fragment was isolated from plasmid pGTE-GFP*BsmBI* by digestion with *BsmBI* and *MluI*. As noted above, the *BsmBI* site has been engineered to generate a GTAC 5’ overhang compatible with an *NcoI* overhang. These fragments were ligated to yield plasmid TpG-N1-GFP. The insertion of GFP resulted in deletion of nt 19-358 from RNA1 and abolished translation of the RdRp; nt 1-19 and nt 359-3204 downstream of GFP remained unchanged. The RNA1 portion of this plasmid is shown schematically in Figure 15.

Plasmids TpGN1-GFPΔSal, TpGN1-GFPΔEag, and TpGN1-GFPΔXho. As a first approach to generating mutant RNA replication templates whose replicability we will test in the *trans* replication system, we deleted three different regions of the RNA1

cDNA from TpG-N1-GFP. The deletions were accomplished by cutting the plasmid with restriction enzymes that were selected because they cut twice in the NoV1 sequence and re-ligating the vector to delete the resulting restriction fragments. The restriction enzymes used were *SalI* (cuts 3' of nt 1549 and 2256), *EagI* (cuts 3' of nt 1212 and 2564), and *XhoI* (cuts 3' of nt 2587 and 3041). TpGN1-GFPΔSal contains a net deletion of nt 1550-2256, TpGN1-GFPΔEag contains a net deletion of nt 1213-2564 of NoV1, and TpGN1-GFPΔXho contains a net deletion of nt 2588-3041. The RNA1 portion of each of these plasmids is shown schematically in Figure 15.

2.3. RNA isolation and Northern blot hybridization analysis

Northern blot hybridization analysis. Total RNA was extracted from plasmid-transformed yeast cells using hot phenol (52) and quantitated by spectrophotometry. The RNA (0.5 μg for detection of positive strands and 2 μg for detection of negative strands) was separated on denaturing formaldehyde-agarose gels and stained with ethidium bromide to allow quantitation of ribosomal RNAs, as described below. The RNA was then transferred to charged nylon membranes (SuPerCharge, Whatman), and analyzed by Northern blot hybridization with strand-specific probes as described previously (33, 41). Strand-specific ^{32}P-labeled RNA probes for NoV subgenomic RNA3 (which also detect RNA1) and NoV RNA2 were generated by *in vitro* transcription from PCR products containing opposed bacteriophage T7 and T3 promoters, as described (52). Probes contained nt 2732 to 3204 of the appropriate sense of NoV RNA1 or nt 1 to 17 and 1100 to 1336 of the appropriate sense NoV RNA2, respectively (39). The results were visualized with a Bio-Rad Personal Molecular Imager and analyzed using Quantity

One 1-D Analysis Software (Bio-Rad Laboratories). Levels of RNA1 and RNA3 replication products were normalized to those of yeast cellular 25S ribosomal RNA (visualized by ethidium bromide staining of the gel before transfer) and are presented as a percentage of the WT values. The relative RNA values from two or three independent experiments (see legends to Figures 10 and 12) are presented as mean values ± standard deviations.

CHAPTER 3

RESULTS

The goal of this research was to identify and investigate *cis*-acting signals important for NoV RNA1 replication. We utilized two different approaches to address this question. In the first approach, the importance of viral UTR's in viral processes (10) led us to investigate the role of the RNA1 3' UTR in its replication. We generated computer predictions of RNA structure in 3'UTR of RNA1 and used site-directed mutagenesis and Northern blot hybridization to assay the contribution of this RNA structure in RNA1 replication. The second approach attempted to map the minimal *cis*-acting RNA elements in RNA1 required for its replication. This involved the creation of a *trans* system of NoV RNA replication, which separated the naturally occurring template and mRNA functions of RNA1 onto two separate molecules. The system would allow us to make changes in the ORF of RNA1 without affecting the function of the RdRp. We used site-directed mutagenesis to create a series of template RNAs which do not produce RdRp and have attempted to produce an RdRp mRNA that cannot replicate its own (endogenous) template. In this chapter we will describe each approach in detail.

3.1. Role in NoV RNA replication of a predicted structure in the RNA1 3'UTR

In the first experimental approach, we wished to investigate whether or not sequences in the 3'UTR of NoV1 promote RNA1 synthesis. This region of RNA1 was selected for further study because the results of two previous studies highlighted the importance of sequences at or near the 3' terminus of genomic RNAs 1 and 2 for RNA replication. First, Albariño et al. (2003) showed that *cis*-acting signals for replication of

FHV genomic RNAs were contained within the 3’ 108 nt of RNA1 and the 3’-terminal 50nt for FHV RNA 2, although the exact sequence element required for RNA replication was not identified (2).

Second, since RNA secondary structures have been shown to be involved in promoting RNA replication of other viruses with RNA genomes (10), we previously investigated the role of RNA secondary structure in replication of NoV RNA2. My colleagues and I showed that a similar region in NoV RNA2 was important for its replication. In that case, we showed that an RNA secondary structure element was predicted to form near the 3’ end of the RNA2 segments of seven different nodaviruses, including NoV. We showed by nuclease mapping that the predicted structure could form in solution.

To determine the functional role of the predicted structure, we used the reverse genetic system for launch of NoV RNA replication in transformed yeast cells to delete the sequences that comprise the structure from a GFP-containing RNA2 replicon and to test the effect of this deletion on RNA replication. Deletion of the stem-loop structure resulted in a severe defect in RNA replication. This deletion appeared to preferentially affect the synthesis of the negative strand replication intermediate, leading to a subsequent decrease in accumulation of positive strands. Finally, a minimal NoV2-GFP replicon whose 3’ end contained only the predicted structure, flanked on each side by 14 nt of RNA2 sequence, including the authentic 3’-terminal 14 nt of RNA2 displayed a reduction in RNA replication. Taken together, these results suggest that the stem-loop structure in the 3’ 50nt of RNA2 is essential for NoV RNA2 replication (Rosskopf, Upton, and Johnson, manuscript in preparation). These lines of experimentation highlighted the

importance of sequences near the 3’ termini and prompted us to ask whether a similar structure might form near the 3’ end of NoV RNA1.

3.1.1. Secondary structure predictions for NoV RNA1

Since many viral RNA replication elements have been shown to form pseudoknot structures, we selected software tools that are able to predict these structures, using the capacities of the UTEP RNA Virtual Laboratory (RNAVLab) when the RNA structure prediction demanded significant amount of time and resources. Therefore, we used three different RNA secondary structure prediction software programs able to predict pseudoknots in RNA, namely NuPack (14, 15), PseudoknotsRE (PknotsRE; (51), and PsuedoknotsRG (PknotsRG; (50) running on the RNAVLab platform, to predict the structures of the 3’ terminal 100, 200, and 300 nucleotides of NoV RNA1.

As shown in Figure 8, all three programs consistently predicted formation of a stem-loop structure in the 3’ UTR of NoV RNA1. This predicted structure involves nt 3162-3177 (NuPack and PknotsRG, shown in Figures 8A and 8B, respectively) or nt 3163-3176 (PknotsRE, shown Figure 8C) for all three nucleotide lengths. The structure contains a 5 bp stem in which nt 3162-3166 base-pair with nt 3173-3177 and a 6 nt loop (nt 3167-3172). In the PknotsRE prediction, the predicted stem was only 4 bp, involving nt 3163-3166 base-pairing to nt 3167-3176 (Figure 8C). These minor inconsistencies in the length of the stem may arise due to slight differences in the algorithms that the different programs use for the predictions. In addition, PknotsRG predicts that the stem-loop structure occurs within the context of a pseudoknot (Figure 8B).

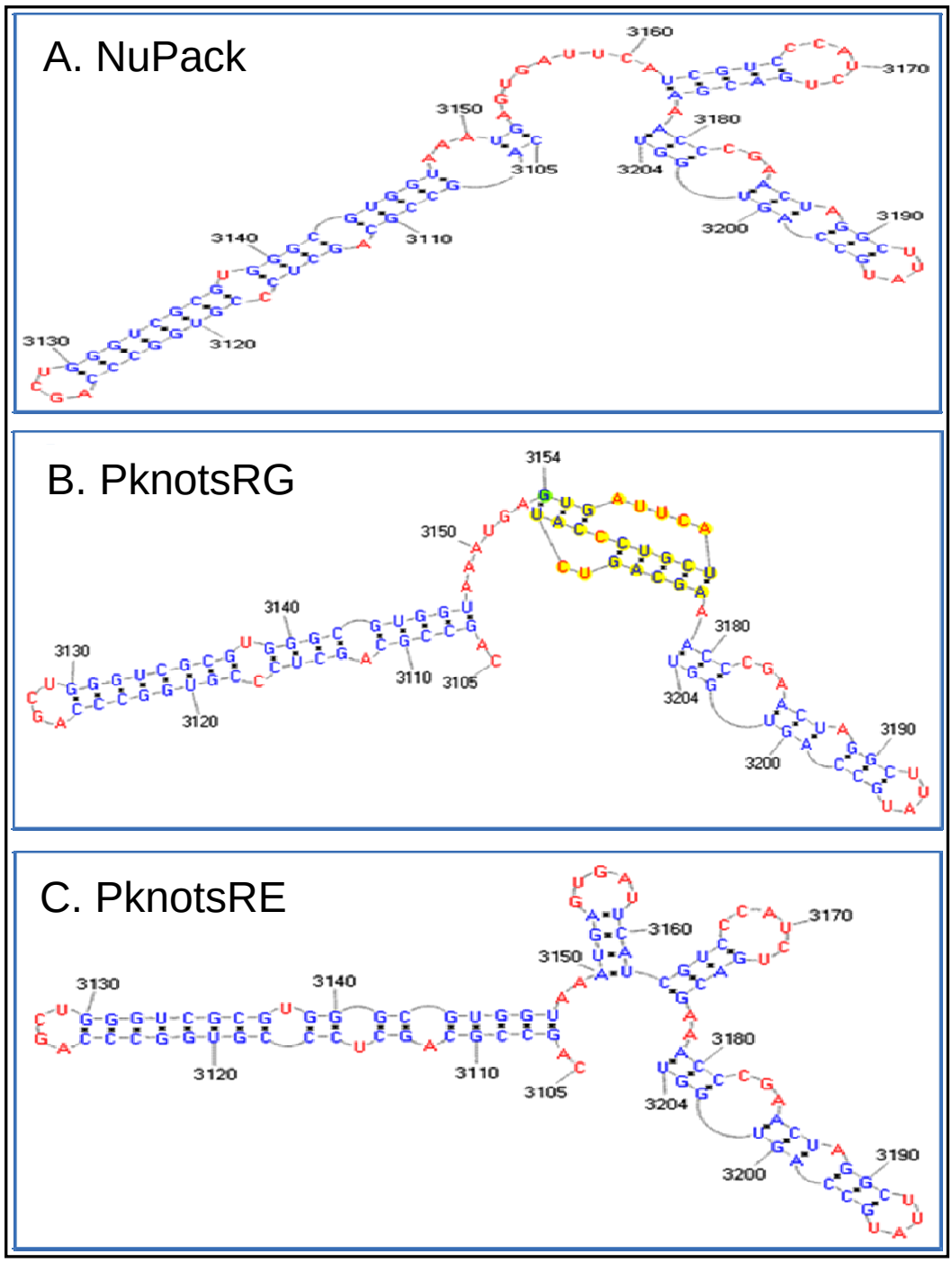

Figure 8. *In silico* prediction of RNA secondary structures. The 3'-terminal 100 nt of NoV RNA1 was used as a substrate for folding by three RNA secondary structure prediction programs (NuPack, PknotsRE, and PknotsRG). All three programs predict a stem loop in the 3'UTR of Nov RNA1. As seen in panels **A** and **B** respectively, NuPack and PknotsRG predict a stem-loop corresponding to nucleotides 3162-3177. PknotsRE, in panel **C**, predicts a stem-loop corresponding nucleotides 3163-3176.

In each case, the predicted loop contained the sequence 5'CCAUCU3'. Interestingly, this sequence is identical to the sequence of the loop that forms near the 3' end of NoV RNA2 (Rosskopf, Upton, and Johnson, manuscript in preparation). As such, it was targeted for further study (see section 3.1.3.). First, however, we tested the effect of deleting the predicted structure entirely.

3.1.2. Deletion of the RNA1 stem-loop results in decreased RNA replication

We hypothesized that this predicted structure is important for NoV RNA1 replication. To test this hypothesis, we used the reverse genetic system for launch of NoV RNA replication in transformed yeast cells (46) to test the role of the predicted RNA1 stem-loop structure in RNA replication. The yeast replication system allows us to launch NoV RNA replication in yeast cells transformed with plasmids that contain cDNA copies of NoV RNA1 and RNA2 under control of an inducible yeast *GAL1* promoter (46). After induction with galactose, primary transcripts of RNA1 and RNA2 are produced. The RNA1 transcripts are translated into the viral RdRp, which replicates RNA1 via negative strand intermediates and synthesizes subgenomic RNA3. When RNA1 and RNA2 are co-transformed into a cell, the RdRp replicates RNA2 *in trans*.

As described in Chapter 2, the yeast strain we use contains deletions in the pathways that synthesize five key nutrients: methionine, histidine, uracil, tryptophan, and leucine. The defects in methionine, histidine, and uracil biosynthesis are complemented by adding these nutrients to the culture medium, while the tryptophan and leucine defects are complemented by transformation with plasmids that contain the yeast *TRP1* and *LEU2* genes, which direct biosynthesis of tryptophan and leucine,

respectively. Therefore, all transformations included a *TRP1*-expressing plasmid (WT or mutant versions of TpG-N1 or YEplac112) and a *LEU2*-expressing plasmid (WT or mutant versions of LpG-N2 or YEp351).

To determine the role of the NoV1 3'SL in the viral replicative cycle, we deleted the sequences that comprise the predicted structure (nt 3162-3177) from the full-length RNA1 cDNA in plasmid TpG-N1 using circular PCR based mutagenesis followed by *DpnI* selection, as described in Chapter 2. Since the mutation is in the 3' UTR, we need not worry about any unintended effect on the RdRp ORF. This deletion is shown schematically in Figure 9.

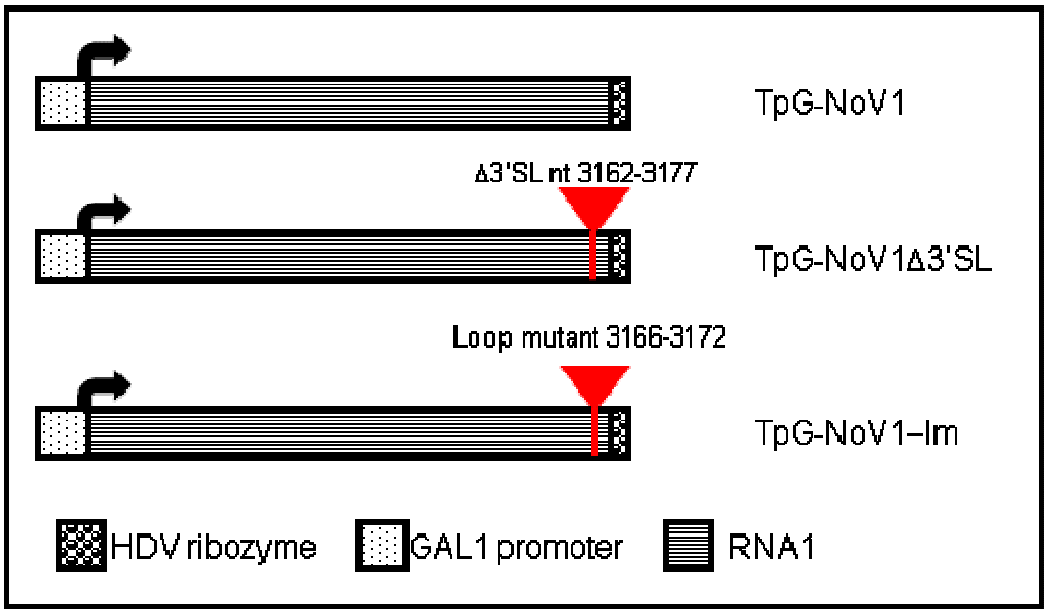

Figure 9. Schematic of NoV1 sequences contained in plasmids TpG-NoV1 and TpG-NoV1Δ3'SL. These plasmids contain cDNA copies of NoV RNA1, under control of the yeast *GAL1* promoter. TpG-NoV1Δ3'SL contains a deletion of the predicted stem-loop corresponding to nucleotides 3162-3177 in RNA1. TpG-NoV1-lm contains a mutation of nt 3166-3172 in the loop portion of the predicted stem-loop from 5' CCCATCT 3' to 5' GGGTAGA 3'.

Yeast cells were transformed with wildtype (WT) or Δ3'SL versions of plasmid TpG-N1, which contains a *TRP1* selectable marker, together with plasmids (YEp351 or LpG-N2) that express the *LEU2* selectable marker. As described above, we used

nutritional selection to ensure that the cells had taken up both plasmids. Transformants still under selection were amplified in liquid culture containing galactose to induce transcription from the *GAL1* promoter. Cells were harvested by centrifugation and total yeast RNA was extracted using a hot phenol method as described (33, 41). Total cellular RNA was separated on a denaturing formaldehyde-agarose gel and transferred to a charged nylon membrane.

NoV RNA replication products were detected by Northern blot hybridization using ^{32}P-labeled probes specific for the positive (Figures 10A, 10C, and 10E) or negative strands (Figures 10B, 10D, and 10F) of RNA3, which also detect RNA1. We detected positive strand monomers of RNA1 and RNA3 when cells were transformed with WT TpG-N1 Figure 10A (lane 2). We also readily detected monomeric and dimeric negative strands of RNA1 and RNA3 (Figure 10B, lane 2). When cells were co-transformed with WT TpG-N1 and the WT RNA2 plasmid LpG-N2, we observed a reduction in the level of RNA1 and RNA3, as described previously (27, 46). The level of positive sense RNA1 was 69% of WT (Figure 10A, lane 5, and Figure 10C), while negative strand RNA1 was 47% of WT (Figure 10B, lane 5, and Figure 10D); the levels of positive and negative strand RNA3 were 74% (Figure 10E) and 51% (Figure 10F) of WT levels, respectively.

However, when the cells were transformed with the stem-loop deletion mutant, TpG-N1Δ3'SL, we detected only 12% of the level of positive strand RNA1 exhibited by WT TpG-NoV1 (Figure 10C), and 7% of the WT level of negative strand RNA1 (Figure 10D).

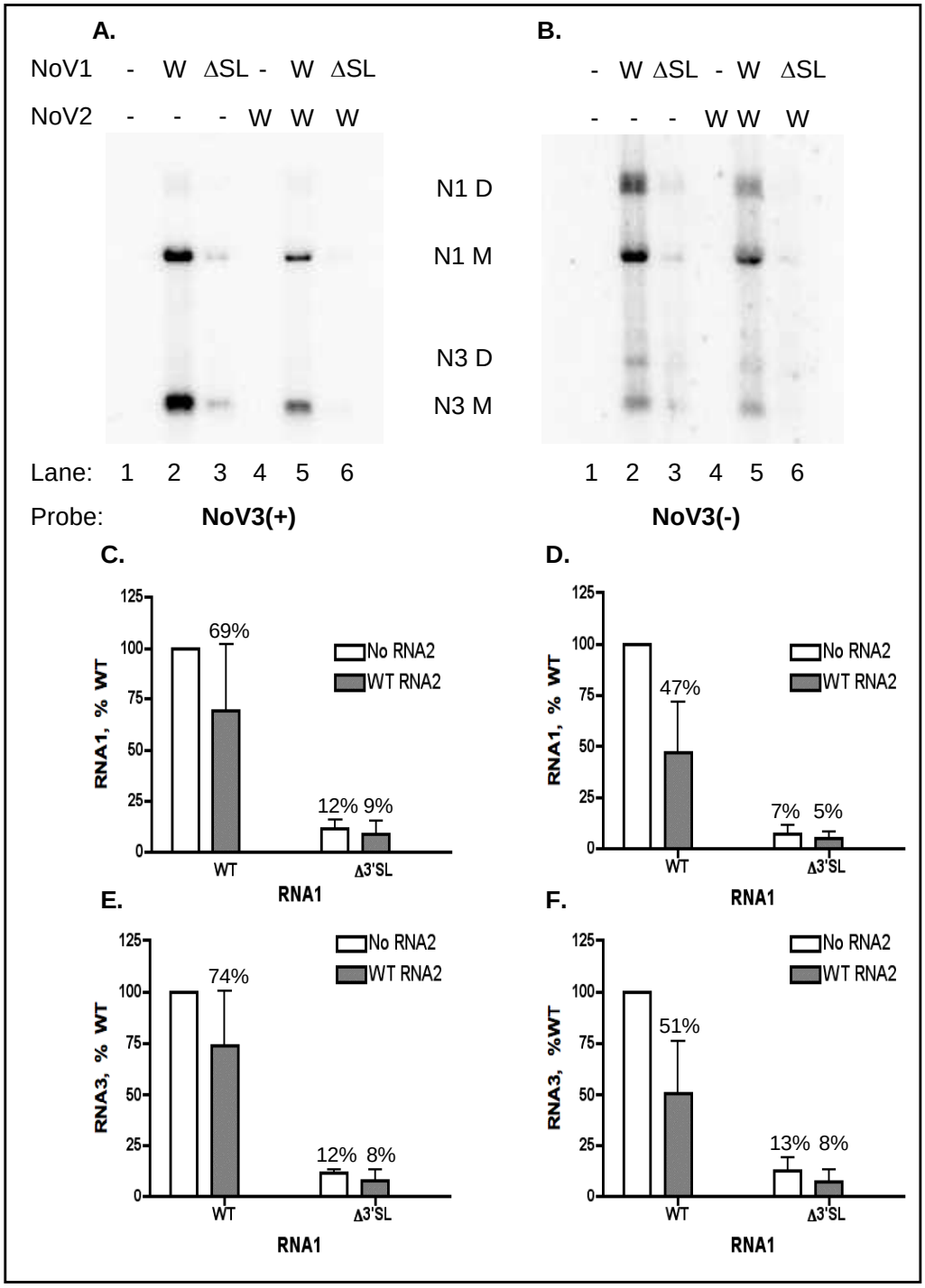

Figure 10. Deletion of RNA1 stem-loop affects RNA replication. Yeast cells were transformed with wildtype or Δ3'SL versions of RNA1 both in the absence or presence of wildtype RNA2. Successful transformants were selected and RNA transcription induced as described in the materials and methods. Northern blot hybridization was carried out using total yeast RNA and using probes specific for positive or negative strands of RNA3 (**Panels A and B**, respectively). **Panel C,** quantitation of RNA1 positive strands; **Panel D,** quantitation of RNA1 negative strands; **Panel E**, quantitation of RNA3 positive strands; **Panel F**, quantitation of RNA3 negative strands. The relative RNA values from three independent experiments are presented as mean values ± standard deviations.

Similarly, this mutant exhibited a reduction in RNA3 levels. We detected 12% of the WT level of positive strand RNA3 (Figure 10E) and 13% the WT level of negative strand RNA3 (Figure 10F). When the cells were co-transformed with TpG-N1Δ3'SL and LpG-N2, we also observed a reduction in levels of RNA1 and RNA3 (Figure 10A lane 6), with positive strand RNA1 at 9% of the WT level (Figure10C) and negative strand RNA1 RNA3 at 5% of the WT level (Figure 10D). RNA3 was similarly reduced in the presence of RNA2 (Figure 10B lane 6): RNA3 positive strands were detected at 8% of the WT level (Figure 10E) and RNA3 negative strands were 8% of the WT (Figure 10F). The N1Δ3'SL mutant showed a severe defect in accumulation of RNA replication products. These results suggest that the sequences comprising the predicted stem-loop are important for the synthesis of negative strand intermediates, which are used as templates to generate further plus strands.

3.1.3. RNA1 replication is affected by mutation of the N1-3'SL loop

The deletion of the nucleotides comprising the predicted stem-loop severely decreased replication of RNA1 and synthesis of RNA3. However, we could not be sure whether it was the complete stem-loop structure itself that was important for RNA replication or one of its component parts; i.e., was only the base-pairing in the stem needed or was the nt sequence in the loop essential for optimal replication? We therefore replaced each of the nucleotides comprising the loop portion of the RNA1 structure with its complement, changing the loop sequence from 5'CCCATCT3' (nt 3166-3172) to 5'GGGTAGA3' (Figure 9). As mentioned above, the 3'SL structure in NoV RNA2, which we found to be crucial for RNA2 replication, contains the same

5’CCCATCT3’ sequence in its loop (Rosskopf, Upton, and Johnson, manuscript in preparation; see section 3.1.2). Because synthesis of RNA2 and RNA3 are counter-regulatory for NoV and FHV (16, 27, 62), and because we observed that both of the predicted 3’SL structures are necessary for replication of their respective RNA segment, we wondered whether these loops played a role in the coordinated synthesis of RNA2 and RNA3. For example, the two loops may interact in some way, such as a base-pairing interaction between the positive-strand loop in RNA1 and the complement of the loop in RNA2. Therefore, we also decided to mutate the loop portion of the 3’SL structure in RNA2 from 5’CCCATCT3’ (nt 1308-1314; Figure 11) to 5’GGGTAGA3’.

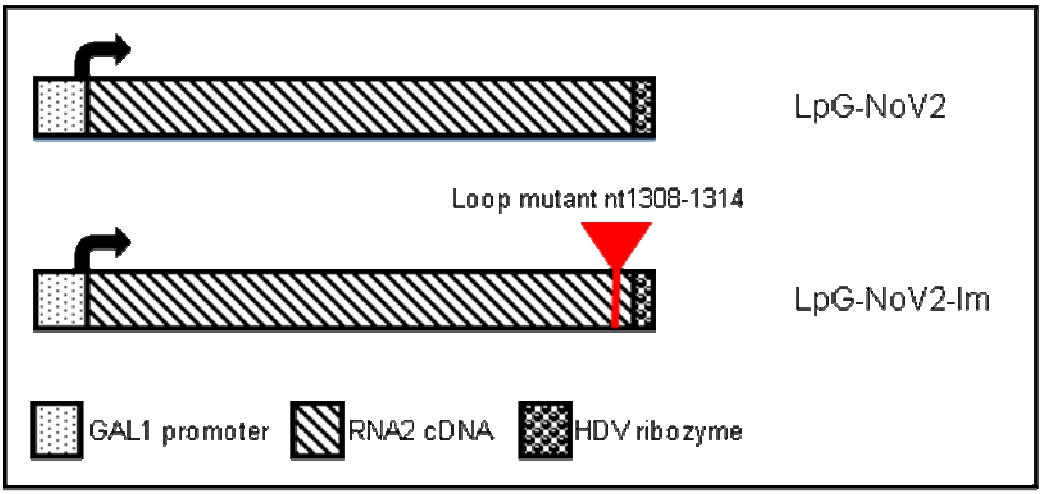

Figure 11. Schematic of the RNA2 cDNA regions of plasmids LpG-NoV2 and LpG-NoV2-lm. These plasmids contain a cDNA copy of NoV RNA2 and both are under the control of the yeast GAL1 promoter. LpG-NoV2-lm contains a mutation in the loop of a predicted stem-loop changing the stem sequence from 5’ CCCATCT 3’ to 5’ GGGTAGA 3’.

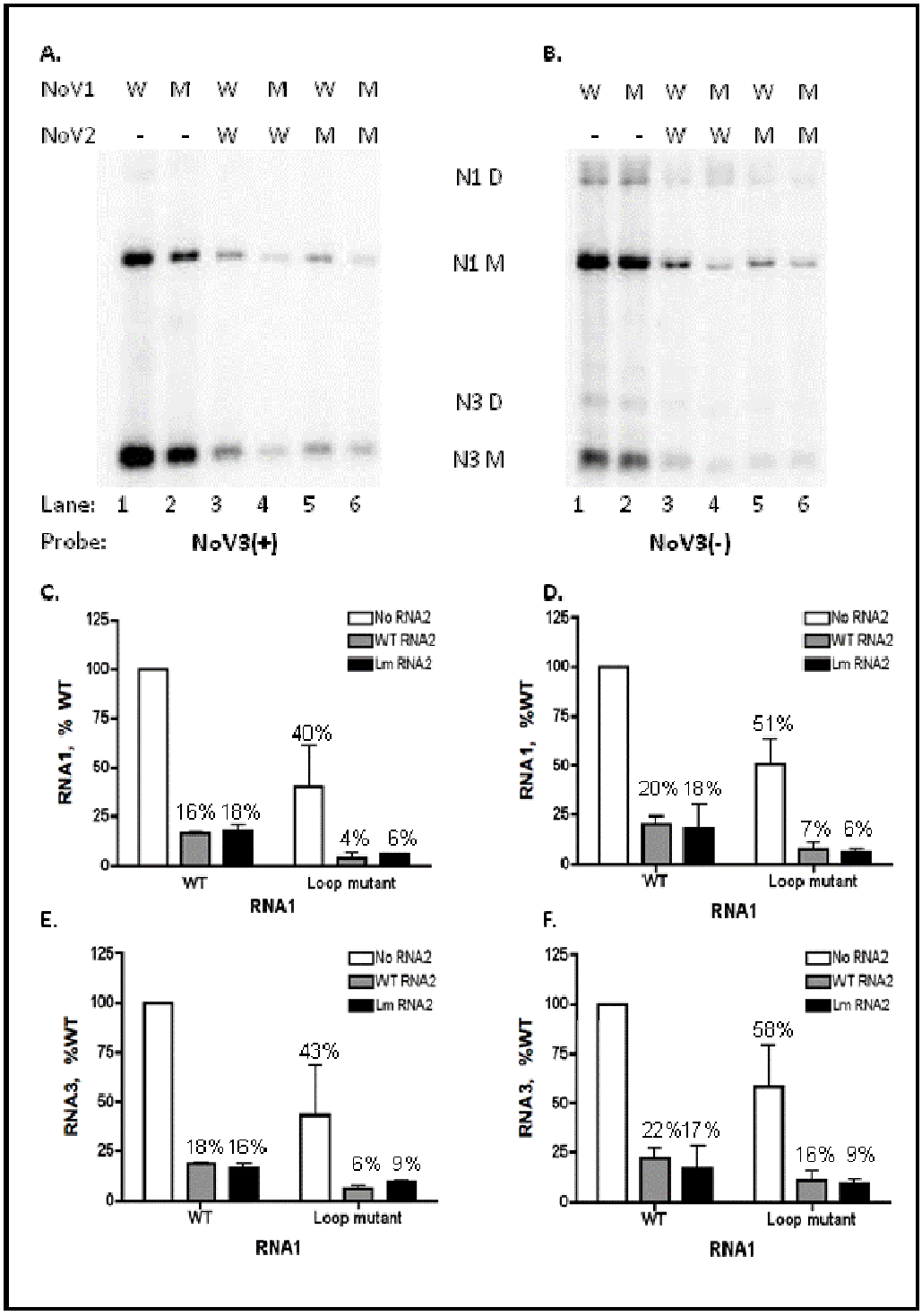

Figure 12. Mutation of RNA1 3'SL loop sequence reduces accumulation of RNA1 and RNA3. Yeast cells were transformed with wildtype (WT) or loop mutant (LM) versions of TpG-N1, either by themselves or in the presence of either wildtype (WT) or loop mutant (LM) versions of LpG-N2. Northern blot hybridization was carried out using total yeast RNA as described in the legend to Figure 10, using probes specific for the positive or negative strands of RNA3 (**panels A and B,** respectively). **Panel C,** quantitation of RNA1 positive strands; **Panel D,** quantitation of RNA1 negative strands; **Panel E**, quantitation of RNA3 positive strands; **Panel F**, quantitation of RNA3 negative strands. The relative RNA values from three independent experiments are presented as mean values ± standard deviations.

We first assayed whether the alterations in the RNA1 stem-loop mutant would affect RNA1 replication. We transformed cells with TpG-N1 or TpG-N1-lm (which contain the *TRP1* gene), either alone or in combination with YEp-351, LpG-N2, or LPG-N2-lm (which contain the *LEU2* gene). Total cellular RNA was separated on a denaturing formaldehyde-agarose gel, transferred to a charged nylon membrane, and analyzed by Northern blot hybridization as before, using the probes that were specific for the positive or negative strands of RNA3.

As before (Figure 10), when WT TpG-N1 was used to transform yeast cells, we could detect monomeric positive strands of RNA1 and RNA3 (Figure 12A, lane 1), and both monomeric and dimeric negative strands (Figure 12B, lane 1). Co-transformation of cells with WT TpG-N1 and the WT RNA2 plasmid LpG-N2, resulted in a reduction in the level of positive and negative strands of RNA1 and RNA3 (Figures 12A, lane 3, and 12B, lane 3, respectively), as before (Figure 10). In this experiment, RNA1 positive strands were detected at 16% of WT (Figure 12C) and negative strands at 20% of WT (Figure 12D). Similarly, RNA3 positive strands were 18% of WT (Figure 12E) and negative strands were 22% of the WT level (Figure 12F). If, instead, the cells were co-transformed with WT TpG-N1 and the RNA2 loop mutant plasmid LpG-N2-lm, no further decrease in RNA1 or RNA3 accumulation was detected (Figure 12A, lane 5, and Figure 12B, lane 5).

In contrast, when the cells were transformed with the plasmid containing the RNA1 loop mutant, TpG-N1-lm, we detected positive strand RNA1 at a level that was 40% of the WT (Figure 12C, lane 2) and negative strands at 51% of WT (Figure 12D). A similar reduction was seen in RNA3 levels: positive strands were detected at a level

that was 43% of WT (Figure 12E) and negative strands at 58% of WT (Figure 12F). The reduction in accumulation of RNA1 and RNA3 was less severe with the loop mutant than that observed with the N1Δ3'SL mutant (compare Figures 10 and 12), perhaps suggesting that sequences in the stem portion of the predicted structure also play an important role in RNA replication.

In the presence of WT LpG-N2, the loop mutant expressed from TpG-N1-lm (Figure 12A, lane 4, and Figure 12B, lane 4) showed the expected reduction in positive and negative strands of RNA1 (Figures 12C and 12D) and RNA3 (Figures 12E and 12F). Similarly, in the presence of the RNA2 loop mutant (Figure 12A, lane 6, and Figure 12B, lane 6), the RNA1 loop mutant also exhibited the expected reduction in and negative strands of RNA1 (Figures 12C and 12D) and RNA3 (Figures 12E and 12F). Thus, in the presence of RNA2, whether WT or the N2 loop mutant, reductions in RNA1 and RNA3 exhibited by the RNA1 loop mutant were not dramatically different than that seen with WT RNA1 in the presence of RNA2 (Figure 10). In addition, mutation of the RNA2 3'SL loop did not affect the accumulation of positive or negative sense RNA1 and RNA3 in the presence of WT or the RNA1 loop mutant (Figure 12A and 12B, lanes 5 and 6).

We next wondered what effect the loop mutants in RNA1 and RNA2 would have on replication of RNA2. Therefore, we prepared duplicate blots from cells transformed with TpG-N1 or TpG-N1-lm (which contain the *TRP1* gene) alone or in combination with YEp-351, LpG-N2, or LPG-N2-lm as described for Figure 12, but this time used probes specific for the positive or negative strands of RNA2 (Figure 13).

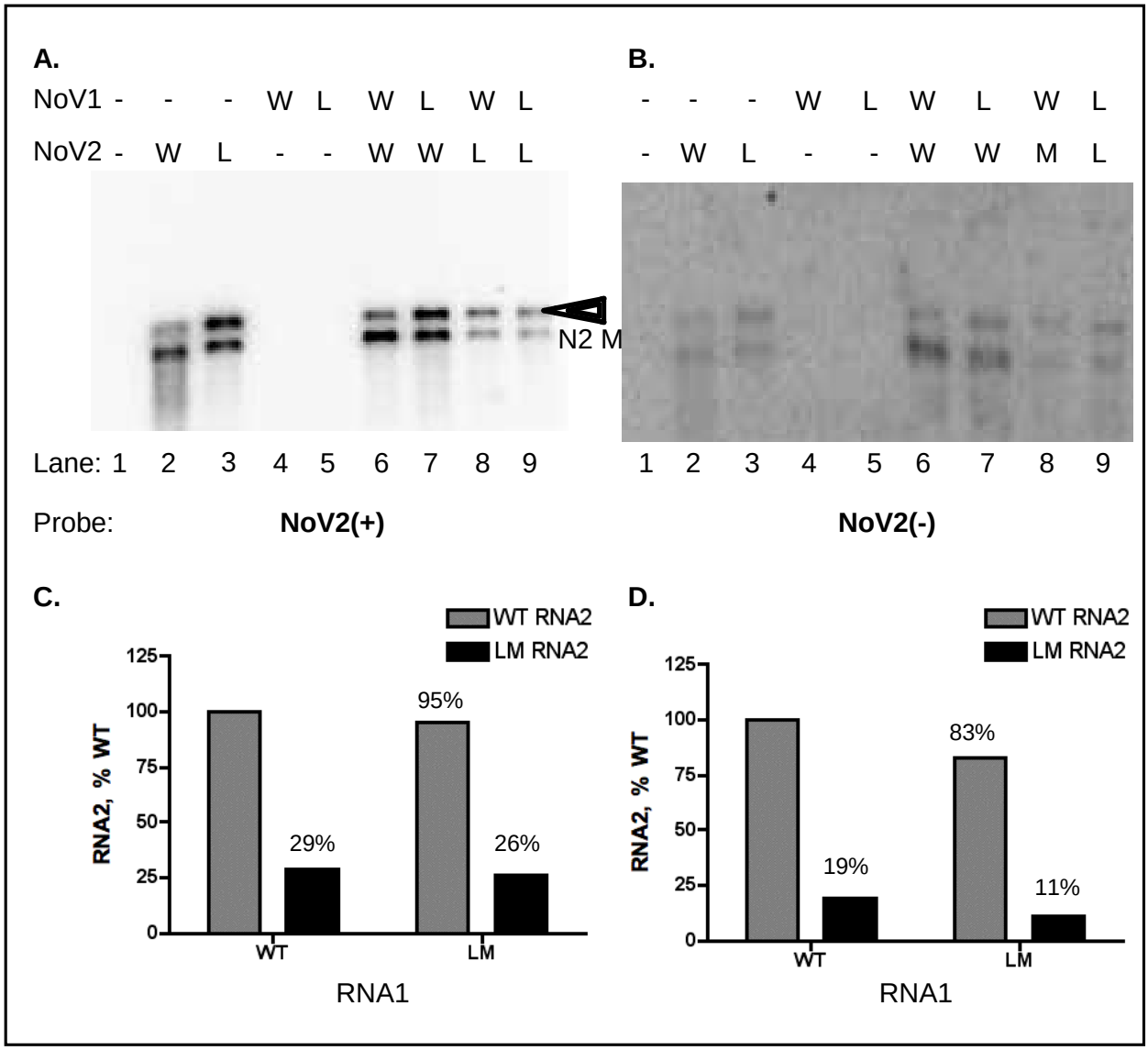

Figure 13. Mutation of loop sequence in RNA2 3'SL reduces its accumulation. Yeast cells were transformed with plasmids expressing WT or loop mutant versions of RNA1, either alone or in the presence of plasmids expressing WT or loop mutant (LM) versions of RNA2. Total yeast RNA was subjected to Northern blot hybridization using probes specific for the positive- or negative- strands of RNA2 (**Panels A and B** respectively). The designation N2M indicates the position of the RNA2 monomer, while the open arrowhead indicates the position of the uncleaved primary transcript of RNA2. **Panel C,** quantitation of RNA2 positive strands; **Panel D**, quantitation of RNA2 negative strands. The relative RNA values from one experiment are presented as mean values.

When cells were transformed with the WT or mutant versions of LpG-N2 in the presence or absence of TpG-N1, we detected two RNA2 species: the expected RNA2 monomer (N2M) and a slightly larger band corresponding to an RNA2 molecule that

contains an uncleaved HDV ribozyme (open arrowhead). The positive strand RNA2 species detected in the absence of the RNA1 plasmid are primary transcripts generated by cellular RNA polymerase II (Figures 13A). Since we do not expect to detect negative strand RNA2 in the absence of the RdRp provided by RNA1, the bands detected in Figure 13B, lanes 2 and 3 may represent cross-reactivity between the positive sense probe and the negative sense primary transcripts. Alternatively, they may represent negative sense primary transcripts generated by cellular RNA *pol II* from a cryptic promoter within the plasmid backbone (see section 3.3.2.).

When cells were co-transformed with WT TpG-N1 and WT LpG-N2, we detected an increase in the levels of the RNA2 monomer in both the positive (Figure 13A, lane 6) and negative (Figure 13B, lane 6) sense. However, on co-transformation of cells with the RNA1 loop mutant TpG-N1-lm and WT LpG-N2 (Figure 13, lane 7), the level of positive sense RNA2 accumulation was 95% (Figure 13C) and negative sense was 83% (Figure 13D), which was not significantly different than RNA2 accumulation in the presence of WT RNA1.

Co-transformation of cells with WT TpG-N1 and the RNA2 loop mutant LpG-N2-lm (Figure 13A, lane 8, and 13B, lane 8) resulted in levels of RNA2 accumulation that were only 29% of WT levels of positive strands (Figure 13C) and 19% of WT levels of negative strands (Figure 13D). Finally, if cells were co-transformed with both loop mutants in plasmids TpG-N1-lm and LpG-N2-lm (Figure 13A, lane 9, and 13B lane 9), we observed only a slight additional reduction in the accumulation of positive and negative strands of RNA2: positive strands were 26% of WT levels (Figure 13C), while negative strands were 11% of WT (Figure 13D). These results suggest that mutating the

loop sequences in the RNA2 3'SL leads to a reduction in RNA2 replication (Figure 13). However, the presence of the RNA1 loop mutant did not alter the accumulation of RNA2 in a significant way as compared to RNA2 levels in the presence of WT RNA1 (Figure 13). Together these data suggest that the predicted stem-loop structures, N13'SL and N23'SL, play a role in the replication of their respective RNAs and that the loop sequences may be involved in synthesis of negative strand replication intermediates. However, it does not appear that the mutation of the loop sequences influences the counter-regulatory relationship between RNA3 and RNA2.

3.2. Extent of RNA1 sequence required for its replication: separation of template and mRNA functions

NoV RNA1 naturally acts as both a template for RNA replication and as an mRNA for translation of the RdRp. This means that changes to the coding region of RNA1 can affect both template properties as well as RdRp function. In order to make mutations that alter only the template and not the RdRp ORF, we used an experimental approach that would allow us to separate the template and mRNA functions onto two different RNA molecules, as was done previously for FHV (35, 47). The *cis* and *trans* replication strategies are summarized schematically in Figure 14. NoV RNA1 replication normally occurs *in cis*, meaning that a molecule of RNA1 is translated to provide viral RdRp that subsequently replicates its own template RNA through negative sense RNA intermediates. In the *trans* replication system, the mRNA and template functions of RNA1 are separated onto two separate molecules, one to provide an RdRp mRNA that cannot function as a template for RNA replication, and the other to provide an RNA replication template that does not encode RdRp. However, when these two molecules

are combined, the RdRp encoded by the mRNA will replicate the template that is provided *in trans*. Once established, this system would allow us to study *cis*-acting replication signals for RNA1 without affecting synthesis of the RdRp. Our efforts to establish this system are described below.

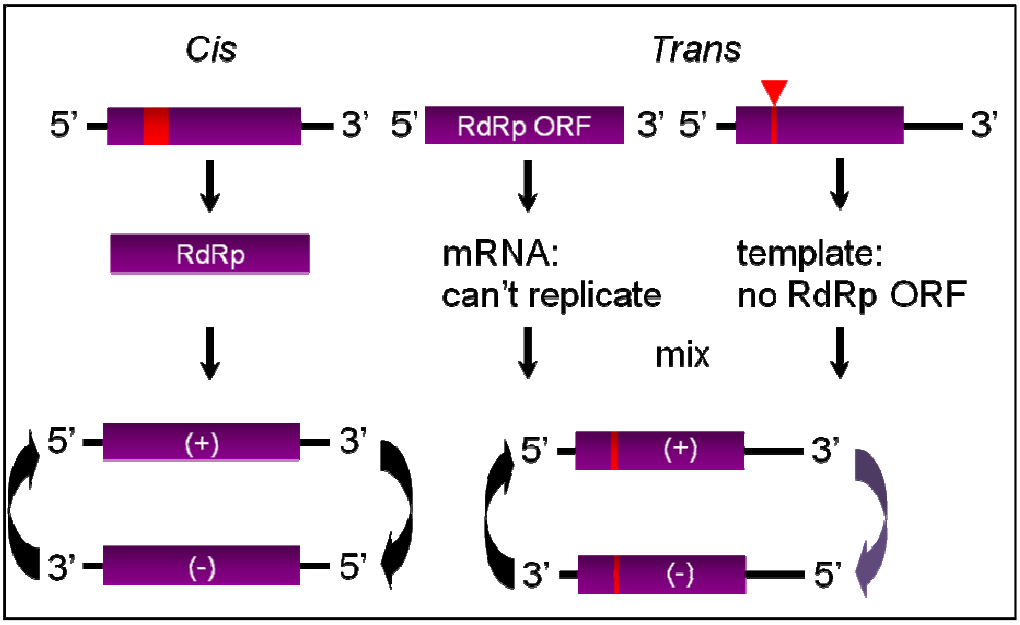

Figure 14. *Cis* versus *trans* RNA replication of NoV RNAs. Schematic representation of how NoV RNA1 normally replicates its RNA in *cis* and the proposed system of RNA1 replication in *trans* in which the mRNA and template functions of NoV RNA1 have been separated onto separate parent molecules.

3.2.1. Production of mutant RNA1 templates

To generate RNA1 templates for use in RNA replication studies, we constructed an expression plasmid based on the RNA1 yeast transcription plasmid TpG-N1 that contains a heterologous central core (GFP) in place of the RdRp ORF. This gave us a plasmid (TpG-N1-GFP) that does not encode the viral RdRp but is still recognized by exogenously supplied RdRp because it retains authentic 5' and 3' termini. The central GFP core supplies an unchanging sequence in the chimeric RNA1 against which we

could direct our probes for Northern blot hybridization. The importance of having templates that cannot provide their own RdRp ensures that changes in the replication of these templates are not due to changes in the RdRp.

This plasmid has been used as the parent of a series of RNA1 mutants. Three additional deletion mutants based on TpG-N1-GFP were constructed by digestion at convenient restriction endonuclease sites and re-ligation. These deletion mutants, TpG-N1GFPΔSal, TpG-N1GFPΔEag, and TpG-N1GFPΔXho, have deletions corresponding to nt 1212-2564, nt 1550-2256, and nt 2588-3041 in NoV RNA1, respectively (Figure 15). We also cloned the DNA fragment containing the N1Δ3'SL deletion into the TpG-N1-GFP background (Figure 15). Each of these four deletion mutations was tested for its ability to serve as a replication template in transformed yeast cells (Figure 17); please see the next section for details. If any of the deleted regions contain nucleotide sequences are involved in NoV RNA1 replication, we should see a decrease in the ability of the corresponding mutant to replicate when combined with the RdRp mRNA plasmid. However, the interpretation of the results will be difficult if the RdRp mRNA retains the ability to serve as a replication template. In the next section we describe several approaches that we have used to generate an NoV RdRp mRNA that cannot be replicated by the RdRp it encodes.

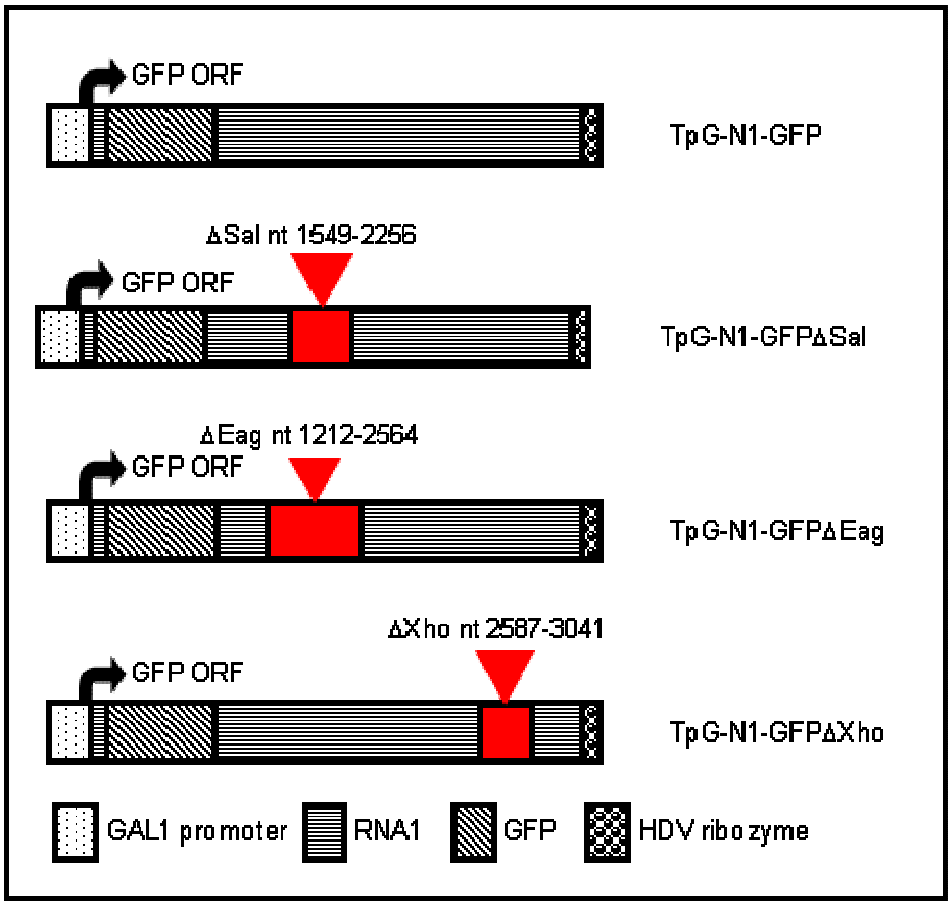

Figure 15. Schematic of template plasmids TpG-N1-GFP, TpG-N1-GFPΔSal, TpG-N1-GFPΔEag, and TpG-N1-GFPΔXho. TpG-N1-GFP contains a GFP ORF that replaces NoV RNA1 nt 20-358. The TpG-N1-GFPΔSal, TpG-N1-GFPΔEag, and TpG-N1-GFPΔXho plasmids contain deletions of NoV RNA1 corresponding to nt 2587-3041, 1212-2564, and 1549-2256 respectively.

3.2.2. RNA1 RdRp mRNA constructs retain activity

The second element required by the *trans* replication system (Figure 14) is the RdRp mRNA expression plasmid. Therefore, we created the LpG-RdRp plasmid, shown schematically in Figure 16, to express RdRp transcripts with a 3 nt deletion at the 5' terminus (nt 1-3 of RNA1) and a complete deletion of the 3'UTR (nt 3154-3204). This plasmid was used to transform yeast cells, either alone or in the presence of the TpG-N1GFP template and its deletion derivatives described in the previous section. Total

yeast RNA was isolated and analyzed by Northern blot hybridization with the negative-strand-specific RNA3 probe as before (Figure 10).

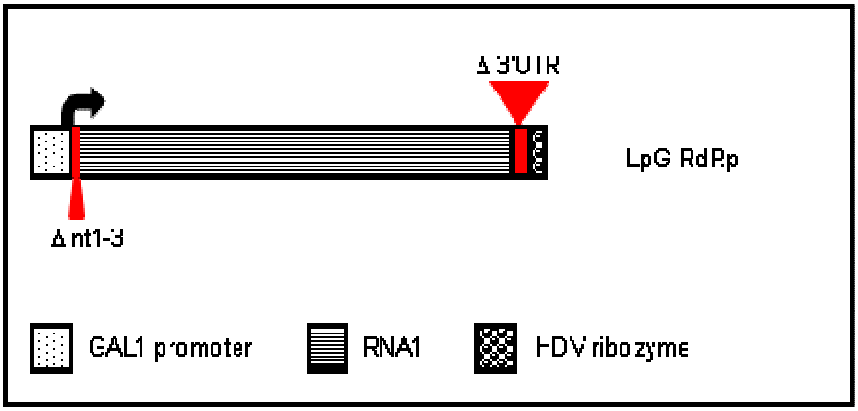

Figure 16. Schematic of plasmid LpG-RdRp. LpG-RdRp contains a deletion of nt 1-3 of RNA1 5'UTR, RNA1 nt 4-3153, and a deletion of the NoV1 3'UTR corresponding to nt 3154-3204 of RNA1 followed by a HDV ribozyme cDNA, cloned into a YEp351 plasmid backbone.

As seen in figure 17, negative sense strands of RNA1 and RNA3 monomers and dimers were not detected in the absence of LpG-RdRp (Figure 17, lanes 1-5). However, in the presence of LpG-RdRp plasmid alone, we detected negative strand monomers and dimers of RNA1 and RNA3 (Figure 17, lane 6). These monomeric and dimeric RNA species were also detected when LpG-RdRp was co-transfected with one of the template constructs: TpG-N1GFP, TpG-N1GFPΔEag, TpG-N1GFPΔXho, or TpG-N1GFPΔSal (Figure 17, lanes 7, 8, 9, and 10 respectively).

However, our ability to detect negative sense RNA1 and RNA3 species in cells transformed with LpG-RdRp alone (Figure 17, lane 6) indicated that the RdRp translated from the LpG-RdRp plasmid could still recognize its endogenous mRNA template and synthesize negative strands. This meant that we were unable to interpret the replication pattern of these mutants (Figure 17), since the RdRp mRNA was still being replicated. Some of the levels of RNA produced by the deletion mutants (Figure

17, lanes 7-10) appear lower than that detected for LpG-RdRp (Figure 17, lane 6). We speculated that this may be due to competition between exogenous and endogenous templates for replication by the RdRp. The ability of the RdRp mRNA to serve as a replication template, even after the deletion of 3nt from the 5' UTR and the entire 3' UTR, led us to believe that further deletions might be needed eliminate its template properties.

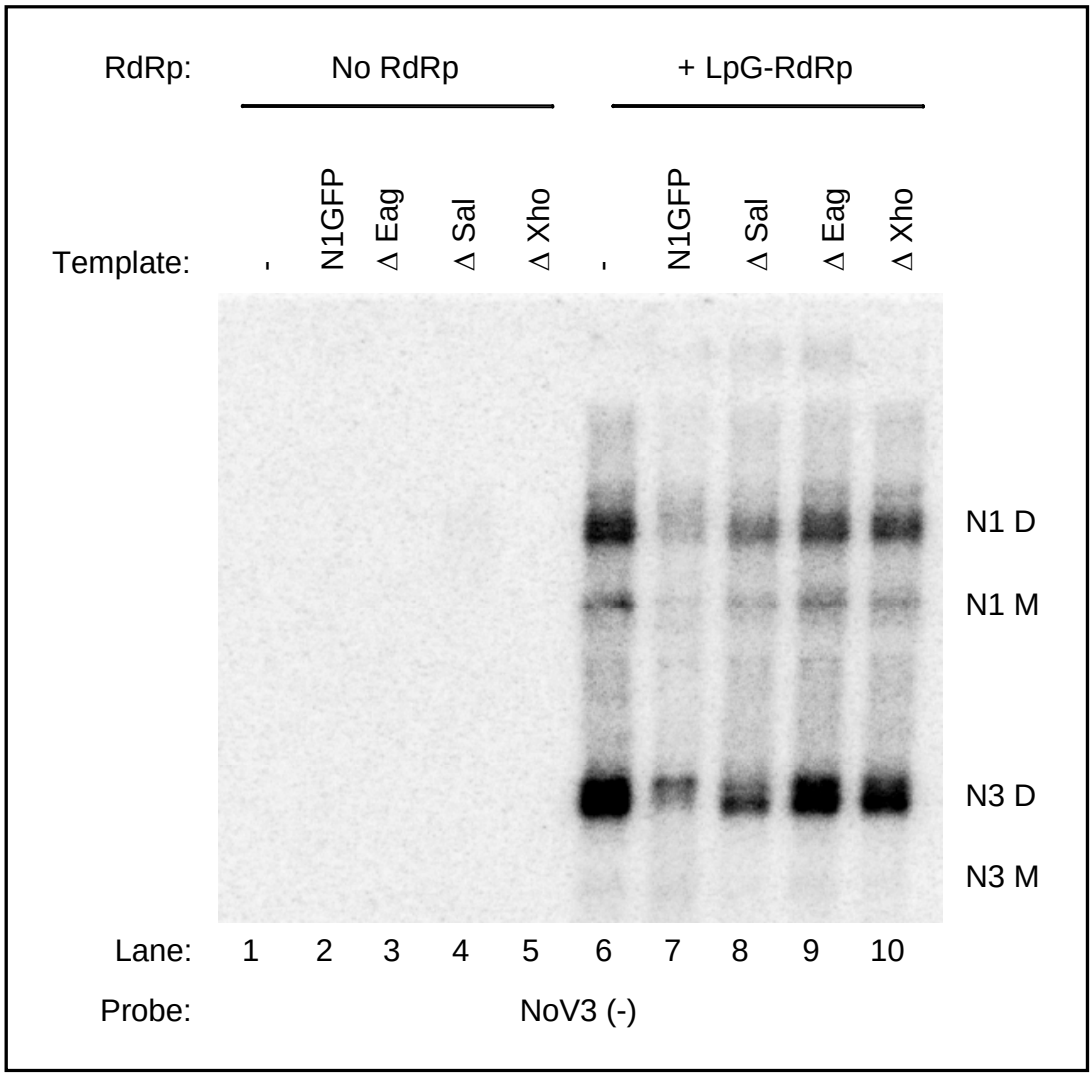

Figure 17. LpG-RdRp retains endogenous template activity. Yeast cells were transformed with the TpGN1-GFP, TpGN1-GFPΔSal, TpGN1-GFPΔEag, and TpGN1-GFPΔXho plasmids in the presence and absence of LpG-RdRp as a source of RdRp. Total yeast RNA was subjected to Northern blot hybridization analysis using a probe specific for the negative strand of RNA3.

We therefore created a series of LpG-RdRp-based plasmids that contained further deletions, in hopes that we could generate an RdRp mRNA that could not serve as a replication template. We made three additional versions of the RdRp mRNA plasmid to determine whether the RdRp mRNA still contained a sequence that acted as a replication signal. First, we considered whether the HDV ribozyme might provide such a signal. The HDV ribozyme forms a pseudoknot-like structure that is required for its efficient self cleavage (43). Since similar RNA structures are important for RNA replication (10), we wished to rule out the possibility that the NoV RdRp could bind to the ribozyme and initiate RNA replication. Therefore, we deleted the ribozyme from LpG-RdRp, resulting in plasmid LpG-RdRpΔRz.

Second, we wondered whether sequences near the C-terminus of the RdRp ORF could still contain a *cis*-acting signal for RNA replication. Considering that we still saw RNA replication in the absence of the 3'UTR, we sought to make further deletions in the RNA1, upstream of the deleted 3'UTR. Using sequence alignment of six nodavirus RdRp's, Johnson *et al.* (2001) showed that the C-terminus of the NoV RdRp extended 20 amino acids beyond the stop codon used by five other nodaviruses (29). We speculated that perhaps this region contained an RNA replication signal and subsequently deleted this region from LpG-RdRp, resulting in plasmid LpG-RdRpΔ20. LpG-RdRpΔ20ΔRz contained both the C-terminal RdRp and ribozyme deletions. These constructs are shown schematically in Figure 18. We then tested the ability of each of these RdRp mRNA's to replicate in yeast (Figure 19).

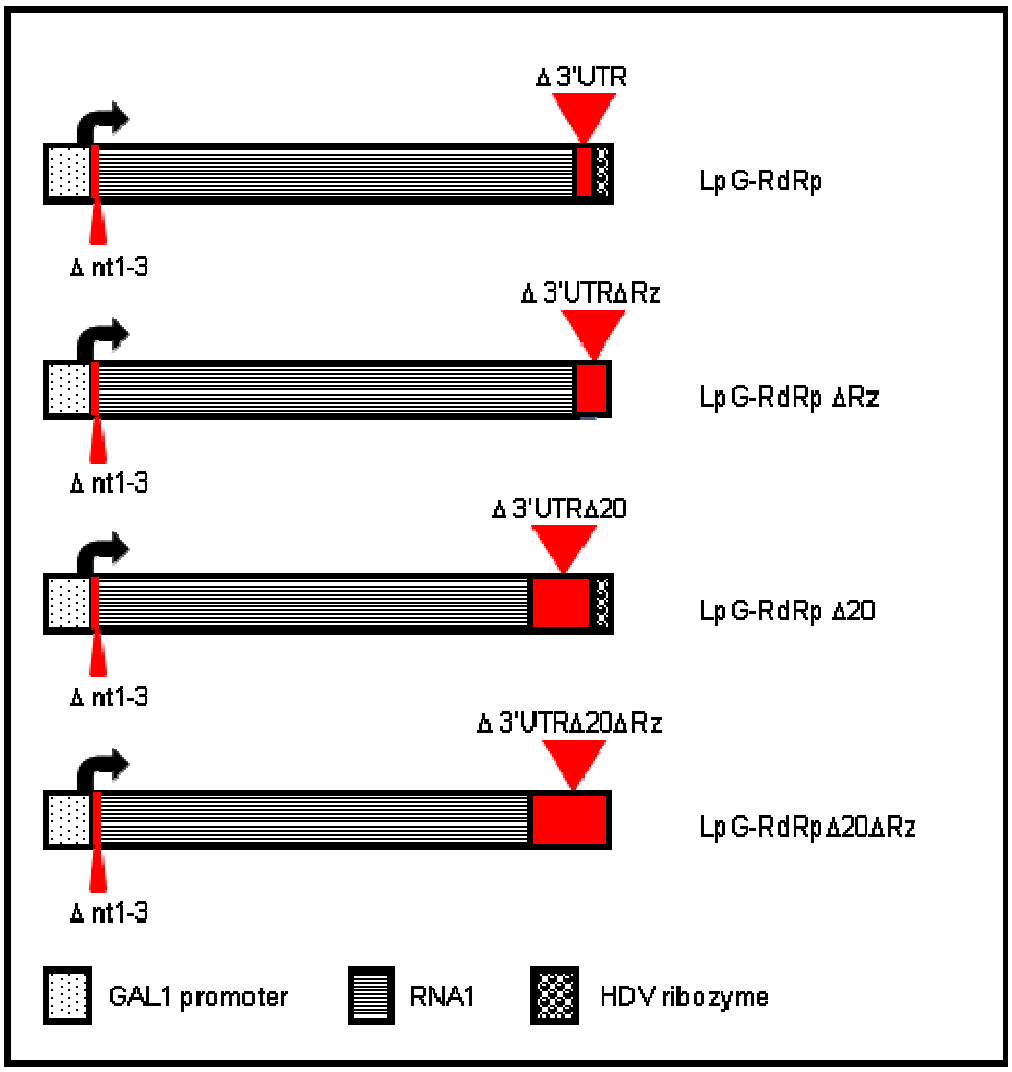

Figure 18. Schematic of plasmids LpG-RdRp, LpG-RdRpΔRz, LpG-RdRpΔ20, and LpG-RdRpΔ20ΔRz. These plasmids are based on LpG-RdRp, which is described in the text and in the legend to Figure 16, but contain deletions designed to stop the ability of the RdRp mRNA to serve as a replication template. The ΔRz mutant has had the HDV ribozyme cDNA deleted. The Δ20 mutant has had the sequence corresponding to the C-terminal 20aa of the RdRp deleted. The Δ20ΔRz version contains deletions of both the HDV ribozyme cDNA and the C-terminal 20aa of the RdRp.

RdRp mRNA plasmids LpG-RdRp, LpG-RdRpΔRz, LpG-RdRpΔ20, and LpG-RdRpΔ20ΔRz were used to transform yeast cells, either alone (Figure 19, lanes 4, 6, 8, and 10) or in the presence of the TpG-N1GFP template (Figure 19, lanes 5, 7, 9, and 11). Total yeast RNA was isolated and analyzed by Northern blot hybridization with the negative-strand-specific RNA3 probe as before. Negative sense RNA1 and RNA3 was

detected for all the constructs, even in the absence of the N1GFP template (Figure 19, lanes 4, 6, 8, and 10). Unfortunately, as before, the ability of the RdRp mRNA's to serve as templates for negative strand RNA synthesis made interpretation of the results impossible.

Interestingly, the negative-strand RNA replication intermediates generated from these constructs were all larger than WT RNA species (Figure 19, compare lane 1 with lanes 4-11). This led us to consider the possibility that there might be a cryptic promoter activity in the backbone of our RdRp expression plasmids. If a cryptic promoter activity resided in the plasmid backbone, downstream of the HDV ribozyme and terminator sequences, it could direct the synthesis of negative sense transcripts that are longer than the RdRp mRNA. By this argument, perhaps we were detecting negative strand primary transcripts rather than RNA replication intermediates in Figures 17 and 19. This interpretation is supported by the observations of Price *et al.* (2002 and 2005), who previously described such a cryptic promoter activity from the YEp351 vector backbone utilized in our RdRp expression plasmids (45, 46).

To rule out possible cryptic promoter activity, we are constructing a new plasmid from which to express the NoV RdRp mRNA. This plasmid, pNA, is based on FHV plasmid pFA, in which the 5' UTR of FHV RNA1 was replaced by a yeast *GAL1* leader and the FHV RNA1 3' UTR was replaced by a yeast *CYC1* polyadenylation signal (35). We have obtained pFA and have used it to redesign NoV RdRp mRNA plasmid. We have generated an mRNA cassette that contains the NoV RdRp ORF, flanked by the *GAL1* leader and the *CYC1* terminator. This NoV RdRp mRNA cassette, which also lacks any HDV ribozyme sequences, will be ligated into a YEp-lac112 vector that has

not previously displayed cryptic promoter activity. This will generate an NoV RdRp mRNA that lacks any 5' or 3' UTR sequences that could be recognized by the RdRp, allowing us to effectively test our TpG-N1-GFP based templates.

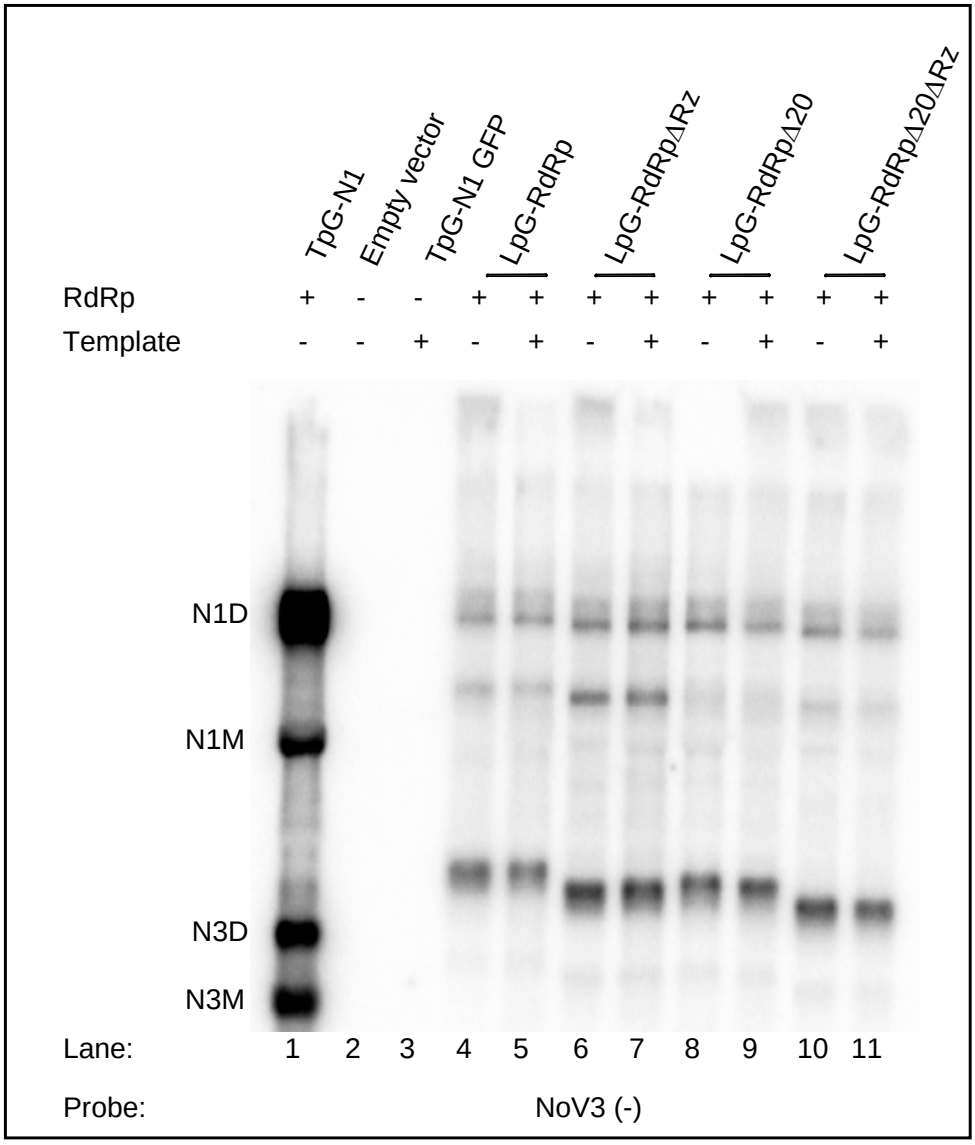

Figure 19. New RdRp mRNA constructs retain ability to replicate endogenous template. Yeast cells were transformed with WT, LpG-RdRpΔRz, LpG-RdRpΔ20, or LpG-RdRpΔ20ΔRz versions of RNA1, either alone or in the presence of the TpGN1-GFP template plasmid. Total yeast RNA was subjected to Northern blot hybridization using a probe specific for the negative strand of RNA3.

CHAPTER 4

SUMMARY AND CONCLUSIONS

4.1 Summary

With these studies, we demonstrated the importance of an RNA secondary structure in the replication of NoV RNA1 and attempted to create a *trans* system of NoV RNA replication that separated the mRNA and template properties of RNA1 onto two different molecules. We have predicted the presence of an RNA structure element in the 3'UTR of NoV RNA1 and shown that it plays an important role in RNA1 replication. We utilized three different computer programs to predict RNA secondary structures in the last 100, 200, and 300nt of NoV RNA1 (Figure 8 for the 100nt predictions). All three programs consistently predicted the presence of a stem-loop in the RNA1 3'UTR for all three nt lengths, which bolstered our confidence in the predictions. The role of RNA secondary structures in RNA replication has not been described in detail for NoV RNA1, but RNA secondary structure has been shown to play a role in FHV RNA3 synthesis (35) and replication of NoV RNA2 (Rosskopf, Upton, and Johnson, manuscript in preparation). Two previous analyses of RNA structures near the 3' termini of seven different nodaviruses RNA2 (BBV, BoV, FHV, NoV, PaV, SJNNV and GGNNV) have shown that this region of RNA2 is structurally conserved (30, 57). This conservation of a small stem-loop structures in nodavirus RNA 3'UTRs led us to investigate the role of this predicted structure in NoV RNA1 replication.

We deleted the nucleotides comprising the predicted structure from a cDNA copy of RNA1 and observed that, when transformed into yeast, this deletion resulted in a

severe defect in RNA1 and RNA3 accumulation (Figure 10). To further define the contribution of loop portion of this structure to RNA replication, we created a cDNA clone of RNA1 and RNA2 containing a mutation of the loop portion of the stem-loop (5' CCCATCT 3' to 5' GGGTAGA 3') that resulted in a reduction (as compared to WT RNA levels) in RNA1 and RNA3 accumulation in cells transformed with TpG-N1-lm (Figure 12) and a reduction in RNA2 accumulation in cells transformed with LpG-N2-lm (Figure 13).

To further define the *cis*-acting signals for RNA1 replication without being limited to mutations that affect only the noncoding regions, we engineered a *trans* replication system for RNA1 that allowed us to separate the template and mRNA properties of RNA1 onto different RNA molecules. This meant that we could make mutations in the RNA1 template and test their effects on RNA replication without affecting the synthesis of the RdRp. Four deletion templates were synthesized in which a portion of the RdRp coding region was replaced with the coding region for green fluorescent protein (GFP), eliminating their ability to synthesize RdRp. The four templates differed from one another by the presence or absence of internal deletions elsewhere in RNA1.

In an effort to generate an RdRp mRNA that could not serve as a replication template, we constructed mutant plasmid LpG-RdRp, which lacked the 3 nt from the RNA1 5'UTR and its entire 3'UTR. When assayed in yeast, the RdRp mRNA synthesized from plasmid LpG-RdRp appeared to have retained the ability to serve as a replication template, as shown by the accumulation of negative sense RNA1 and RNA3 molecules (Figure 17). Therefore, we generated three additional constructs based on the LpG-RdRp plasmid: LpG-RdRpΔRz, LpG-RdRpΔ20, and LpG-RdRpΔ20ΔRz. These

constructs differed from LpG-RdRp in that they contained additional deletions at the 3' end of the RdRp mRNA. When tested in yeast, each construct (including LpG-RdRp) again appeared to retain its endogenous template activity, since each generated negative strand RNA species that hybridized to the RNA3-specifc probe (Figure 19). However, the observation that these RNA species were all longer than expected led us to conclude that they might actually represent negative sense primary transcripts generated from a cryptic promoter activity in the plasmid rather than replication products. It is clear that we must revise our strategy in such a way to eliminate the apparent cryptic promoter activity.

4.2. Conclusions

The role of RNA secondary structures in RNA replication has not been previously addressed for NoV RNA1. Previous predictions of RNA secondary structure in the 3'UTRs of nodavirus RNA2 segments predicted the presence of conserved stem-loop structures for BBV, BoV, FHV, NoV, PaV, SJNNV, and GGNNV RNA2 (30, 57). Subsequent study of the stem-loop in of NoV RNA2 demonstrated that it was important in the synthesis of negative strand replication intermediates (Rosskopf, Upton, and Johnson, manuscript in preparation), Our prediction of a stem-loop in the 3'UTR of RNA1 led us to wonder whether the stem loop in RNA1 would also play a role in negative strand RNA synthesis.

Deletion of the predicted N1 3'SL resulted in a profound deficiency in RNA1 replication (Figure 10). We detected RNA1 at a level that was 12% of WT in the positive sense (Figure 10C) and 7% WT in the negative sense (Figure 10D). A similar reduction

in RNA accumulation was seen in RNA3 (Figure 10), with levels being 12% of WT in positive sense RNA3 (Figure 10E) and 13% of WT in negative sense RNA3 (Figure 10F). The fact that NoV replicates its RNA through negative strand intermediates led us to believe that the reduction in RNA1 and RNA3 is due to a deficiency in negative strand synthesis. We believe this is true because a deficiency in minus strand synthesis would lead to a lack of positive strand accumulation. We therefore speculate that this stem-loop may represent at least a part of a hypothetical promoter used to initiate RNA1 negative strand synthesis. If instead this N1Δ3'SL deletion mutant exhibited a primary defect in positive strand synthesis, we would expect to see an accumulation of negative sense replication intermediates, but no corresponding increase in positive strand RNA replication products.

When WT RNA1 replicated in the presence of RNA2, we observed a reduction of RNA1 replication and RNA3 synthesis. Positive strand accumulation for RNA1 was 69% of the WT level and 47% of WT for negative strands, while positive strand RNA3 was 74% of WT and negative strands were 51% of the WT levels. This reduction in RNA accumulation has been observed previously for NoV RNA1 replication in the presence of RNA2 (27) and may represent competition between the viral RNAs for RdRp.

When the N1Δ3'SL mutant replicated in the presence of RNA2, RNA1 levels were 9% of WT for positive strands (Figure 10C) and 5% of WT for the negative strands (Figure 10D) and RNA3 levels were 8% of WT in the positive sense (Figure 10E) and 8% of WT in the negative sense (Figure 10F). This decrease was not statistically different from the RNA1 and RNA3 levels exhibited when Δ3'SL mutant was replicating in the absence of RNA2 (Figures 10C-10F), indicating that RNA2 did not further reduce

RNA1 and RNA3 synthesis for the N1Δ3'SL deletion mutant. Even though this mutant exhibited diminished RNA replication, low levels of negative strand synthesis were still detectable. This residual activity implies that other RNA sequences or structures may play a role in the negative strand RNA synthesis. One possibility is that long range interactions between nucleotides in RNA1 may play a role in its replication. Such long range interactions have been shown to play a role in FHV RNA3 accumulation (35). Is a long-range base pairing interaction possible in NoV RNA1? A preliminary search using bioinformatics software with the sequence 5'CCATCT3', which is contained in the predicted N13'SL loop, has revealed the presence of a complementary sequence, 3'AGATGG5' (nt 3050-3045), to which the loop nucleotides could base pair (Rosskopf and Betancourt, unpublished observation). This search also revealed a second region, 3'AGATG5' (nt 2585-2581), that is complementary to an overlapping sequence that contains only five of the seven loop nucleotides, 5'CATCT3'. These predictions show that long range interactions involving the predicted N1-3'SL are possible. We also cannot rule out the possibility that higher order RNA structures formed by long range nucleotide interactions could play other roles in the nodavirus replicative cycle, such as translational regulation.

We wondered whether the entire stem-loop structure was important for RNA1 negative strand synthesis or whether the stem or the loop sequences alone were sufficient. Therefore, we mutated the sequence of the loop region from 5'CCCATCT3' to 5'GGGTAGA3' by replacing each nt with its complement. When replicating alone, the RNA1 loop mutant had positive sense RNA1 levels 40% of WT (Figure 12C) and negative sense RNA1 levels 51% of WT (Figure 12D). RNA3 levels were similar in that

the positive sense was 43% of WT (Figure 12E) and the negative sense levels were 58% of WT (Figure 12F). These reductions in RNA accumulation were significant and demonstrated the importance of the loop sequence in RNA1 replication. The reduction in RNA levels compared to WT was less severe than seen in the loop deletion (Figure 10), indicating the loop did not comprise the entire signal for negative strand RNA synthesis.

The mutation of the RNA1 loop (N1LM) also led to significant reduction in RNA1 and RNA3 levels when the mutant replicated in the presence of RNA2, but the reduction was similar to the reduction seen with WT RNA1 and RNA2. In the presence of WT RNA1 and WT RNA2, positive sense RNA1 levels were 16% of WT RNA1 alone (Figure 12C) and negative sense RNA1 was 20% of WT alone (Figure 12D). RNA3 levels, as compared to WT RNA1 replicating alone, followed a similar pattern with positive sense RNA3 being 18% of WT alone and negative sense transcripts 22% of WT alone. The N1LM, replicating in the presence of WT RNA2, displayed a similar reduction in RNA1 and RNA3 accumulation in both the positive and negative sense (Figure 12C-12F).

As mentioned in Chapter 3, we noticed that the RNA1 loop sequence was identical to the loop sequence in the 3'SL structure in RNA2 that we previously showed to be important for RNA2 replication. We considered the possibility that one loop sequence (e.g., the positive strand N1-3'SL) might be able to base pair with the complement of the other (e.g., the negative strand N2-3'SL). To test this possibility, we similarly mutated the RNA2 loop sequence from 5'CCCATCT3' to 5'GGGTAGA3' and tested its effect on replication of RNA1 and RNA2. This mutation (N2LM) is expected to disrupt the hypothetical base pairing between the RNA1 and RNA2 loops, but to restore

complementarity with the RNA1 loop mutant, N1LM. Mutation of the RNA2 loop significantly reduced RNA2 replication (Figure 13). When WT RNA1 was used to support replication of the N2LM, accumulation of positive strand RNA2 was only 29% of WT RNA2 (Figure 13C) and negative strands were 19% of the WT RNA2 levels (Figure 13D). These results suggest that the 3'SL loop in NoV RNA2 was important for its replication.

In the converse experiment, the N1LM was used to support replication of either the WT or LM versions of RNA2. N1LM had relatively little effect on RNA2 replication. When N1LM supported WT RNA2, positive strand RNA2 was 95% of the level seen with WT RNA1 (Figure 13C) and negative strands were 83% of the level seen with WT RNA1 (Figure 13D). However, when N1LM supported the N2LM mutant, positive strand RNA2 levels were 26% of WT (Figure 13C) and negative strands were 11% of WT (Figure 13D). This is very similar to the RNA2 levels seen when N2LM was supported with WT RNA1, suggesting that changes in the loop of N1-3'SL had no effect on RNA2 replication. Similarly, we did not observe a large change in the accumulation of RNA1 and RNA3 when cells were co-transformed with both mutants (Figure 13).

The RNA2 loop mutant did not further reduce the levels of RNA1 and RNA3 when compared to WT RNA2; but it did reduce the amount of RNA2 accumulation as compared to WT when co-transformed into yeast cells with either the WT RNA1 or RNA1-lm (Figure 13). Together these results led us to believe that loop sequences in RNA1 and RNA2 are required for replication of the respective genome segment, but they do not appear to influence the counter-regulatory mechanism between RNA3 and RNA2 (16, 27, 62).

We wondered whether there might be additional *cis*-acting signals that were important for NoV RNA1 replication. Some of these signals, we reasoned, might be contained in the RdRp ORF portion of RNA1. This meant that we needed a way to separate the mRNA function from the template function of RNA1 so we could make changes in the ORF that would not alter the RdRp. To accomplish this, we set up a *trans* replication system for RNA1. This system utilizes two separate RNA molecules to accomplish what NoV RNA1 naturally accomplishes with one: an RdRp provided from a RdRp mRNA that cannot serve as a replication template and a template RNA1 that does not provide RdRp.

We first created an RNA1 template, TpG-N1GFP, that contained a heterologous central core (GFP) in place of the RdRp ORF RNA1 and authentic RNA1 5' and 3' termini (as described in section 3.2.1). This provided us with a template that could not produce RdRp and that contained an unchanging region of RNA, the GFP sequence, against which we could design probes for detection of replication products via Northern blot hybridization. We created three additional template mutants that contained deletions in the RNA1 sequences in TpG-N1GFP – these are shown schematically in Figure 15. To test the replication of these templates, we needed to generate an RdRp mRNA that could not serve as a replication template.

We reasoned that many replication determinants must lie at the termini. Therefore, our first attempt to generate an RdRp mRNA involved deleting a small portion from the 5'UTR (nt 1-3) and the entire 3'UTR (nt 3154-3204), resulting in plasmid LpG-RdRp. When transfected into yeast, either alone or in the presence of the replication templates described above, we detected negative sense RNA1 and RNA3 by

Northern blot hybridization, suggesting that the RdRp mRNA could still act as an endogenous template (Figure 17). The deletion templates TpGN1-GFPΔEagI, TpGN1-GFPΔXhoI, and TpGN1-GFPΔSalI, were also tested in the presence of LpG-RdRp (Figure 17). However, the apparent ability of the RdRp mRNA produced by LpG-RdRp to serve as a replication template makes interpretation of these results impossible.

We then considered the following possibilities: that the RdRp could somehow recognize the secondary structure adopted by the HDV ribozyme as a replication signal and that the 20aa C-terminus of the NoV RdRp, which is not conserved among other nodavirus RdRps (29), might contain an RNA replication signal. To test these possibilities, we constructed three variants of plasmid LpG-RdRp that contained deletions of the ribozyme (LpG-RdRpΔRz) or the potential C-terminal extension of the RdRp ORF (LpG-RdRpΔ20) or both deletions together (LpG-RdRpΔ20ΔRz), in hopes that one or more of these variants might abrogate the mRNA's ability to serve as an endogenous replication template.

When these RdRp constructs were used to transform yeast cells, we detected what we interpreted to be negative strands of RNA1 and RNA3. These results suggested that the mutant RdRp mRNA constructs could still serve as replication templates (Figure 19). As before, although these RdRp constructs were tested for their ability to support replication of the TpGN1-GFP template (Figure 19), the endogenous template activity of the RdRp mRNA's made interpretation of these results impossible. For all four of these RdRp constructs, the negative strand RNA species detected were consistently larger than authentic RNA replication products and they occurred at lower levels than those seen in the presence of self-replicating NoV1 (Figure 19). The ability

of these mutants to generate negative sense transcripts without the 3'UTR that were larger than authentic RNA replication products was unexpected. Price *et al.* (2005) demonstrated negative sense primary transcripts of NoV RNA2 could be synthesized from plasmid LpG-NoV2 by cellular RNA polymerase that recognized a cryptic promoter activity in the vector backbone; similar results were seen with FHV RNA2 in the same plasmid backbone (45, 47). These results led us to believe that cryptic promoter activity may be present in the YEp351 vector backbone of our constructs. In that case, the negative sense RNA1 and RNA3 species that we detected by Northern blot hybridization might actually represent negative sense primary transcripts rather than RNA replication products. To address this possibility, we will construct the next generation of NoV RdRp mRNAs in a YEplac112 backbone, which has not been shown to contain a cryptic promoter. We have also designed a new strategy for generating the RdRp mRNA. We will replace the entire RNA1 5'UTR with the yeast *GAL1* leader sequence and the 3'UTR with the yeast *CYC1* polyadenylation signal, to generate pNA. This strategy has been used successfully by Lindenbach, *et al.*, (2002) to express an mRNA of the FHV RdRp (35). Hopefully this approach will allow us to generate an RdRp mRNA for NoV that cannot serve as an endogenous template.

In conclusion, we predicted the presence of a stem-loop in the 3'UTR of NoV RNA1 (N1-3'SL) and have demonstrated that it is involved in negative strand RNA1 synthesis. While it may comprise part of the promoter used to initiate negative strand synthesis, it does not comprise the entire promoter. We have also shown that either deleting the entire N1-3'SL or altering its loop sequence greatly reduces the accumulation of RNA1 and RNA3 negative strands, leading to a decrease in positive

strand synthesis. In addition, altering the analogous loop sequence of the RNA2 3'SL reduced the levels of RNA2. These studies detail a *cis*-acting element involved in NoV RNA1 replication and hint at a possible mechanism for NoV RNA replication by the similarities in RNA secondary structures in the 3'UTRs of NoV RNA1 and RNA2 determined to be important for negative strand RNA synthesis.

Finally, we have created four RNA1 templates for our NoV RNA1 *trans* replication system. The RdRp mRNAs we have created to date are still being recognized as templates by the NoV RdRp. We believe that this may be due to cryptic promoter activity in our vector backbone; and we are currently working on another mRNA construct that we believe will address this issue.

LIST OF REFERENCES

1. **Ahlquist, P., A. O. Noueiry, W. M. Lee, D. B. Kushner, and B. T. Dye.** 2003. Host factors in positive-strand RNA virus genome replication. J Virol **77:**8181-6.
2. **Albariño, C. G., L. D. Eckerle, and L. A. Ball.** 2003. The cis-acting replication signal at the 3' end of Flock House virus RNA2 is RNA3-dependent. Virology **311:**181-91.
3. **Albariño, C. G., B. D. Price, L. D. Eckerle, and L. A. Ball.** 2001. Characterization and template properties of RNA dimers generated during flock house virus RNA replication. Virology **289:**269-82.
4. **Angeletti, P. C., K. Kim, F. J. Fernandes, and P. F. Lambert.** 2002. Stable replication of papillomavirus genomes in Saccharomyces cerevisiae. J Virol **76:**3350-8.
5. **Bailey, L., and H. A. Scott.** 1973. The pathogenicity of Nodamura virus for insects. Nature **241:**545.
6. **Ball, L. A.** 1992. Cellular expression of a functional nodavirus RNA replicon from vaccinia virus vectors. J Virol **66:**2335-45.
7. **Ball, L. A., J. M. Amann, and B. K. Garrett.** 1992. Replication of Nodamura virus after transfection of viral RNA into mammalian cells in culture. J Virol **66:**2326-34.
8. **Ball, L. A., B. Wohlrab, and Y. Li.** 1994. Nodavirus RNA replication: mechanism and harnessing to vaccinia virus recombinants. Arch Virol Suppl **9:**407-16.
9. **Brachmann, C. B., A. Davies, G. J. Cost, E. Caputo, J. Li, P. Hieter, and J. D. Boeke.** 1998. Designer deletion strains derived from Saccharomyces cerevisiae

S288C: a useful set of strains and plasmids for PCR-mediated gene disruption and other applications. Yeast **14:**115-32.

10. **Brierley, I., S. Pennell, and R. J. Gilbert.** 2007. Viral RNA pseudoknots: versatile motifs in gene expression and replication. Nat Rev Microbiol **5:**598-610.
11. **Buchholz, U. J., S. Finke, and K.-K. Conzelmann.** 1999. Generation of bovine respiratory syncytial virus (BRSV) from cDNA: BRSV NS2 is not essential for virus replication in tissue culture, and the human RSV leader region acts as a functional BRSV genome promoter. J. Virol. **73:**251-259.
12. **Castorena, K. M., S. A. Weeks, K. A. Stapleford, A. M. Cadwallader, and D. J. Miller.** 2007. A functional heat shock protein 90 chaperone is essential for efficient flock house virus RNA polymerase synthesis in Drosophila cells. J Virol **81:**8412-20.
13. **Chao, J. A., J. H. Lee, B. R. Chapados, E. W. Debler, A. Schneemann, and J. R. Williamson.** 2005. Dual modes of RNA-silencing suppression by Flock House virus protein B2. Nat Struct Mol Biol **12:**952-7.
14. **Dirks, R. M., and N. A. Pierce.** 2004. An algorithm for computing nucleic acid base-pairing probabilities including pseudoknots. J Comput Chem **25:**1295-304.
15. **Dirks, R. M., and N. A. Pierce.** 2003. A partition function algorithm for nucleic acid secondary structure including pseudoknots. J Comput Chem **24:**1664-77.
16. **Eckerle, L. D., C. G. Albariño, and L. A. Ball.** 2003. Flock House virus subgenomic RNA3 is replicated and its replication correlates with transactivation of RNA2. Virology **317:**95-108.

17. **Fenner, B. J., R. Thiagarajan, H. K. Chua, and J. Kwang.** 2006. Betanodavirus B2 is an RNA interference antagonist that facilitates intracellular viral RNA accumulation. J Virol **80:**85-94.

18. **Garzon, S., G. Charpentier, and E. Kurstak.** 1978. Morphogenesis of the nodamura virus in the larbae of the lepidopteran Galleria mellonella (L.). Arch Virol **56:**61-76.

19. **Garzon, S., H. Strykowski, and G. Charpentier.** 1990. Implication of mitochondria in the replication of Nodamura virus in larvae of the Lepidoptera, Galleria mellonella (L.) and in suckling mice. Arch Virol **113:**165-76.

20. **Gietz, R. D., and A. Sugino.** 1988. New yeast-Escherichia coli shuttle vectors constructed with in vitro mutagenized yeast genes lacking six-base pair restriction sites. Gene **74:**527-34.

21. **Guarino, L. A., and P. Kaesberg.** 1981. Isolation and Characterization of an RNA-Dependent RNA Polymerase from Black Beetle Virus-Infected Drosophila melanogaster Cells. J Virol **40:**379-386.

22. **Hill, J. E., A. M. Myers, T. J. Koerner, and A. Tzagoloff.** 1986. Yeast/E. coli shuttle vectors with multiple unique restriction sites. Yeast **2:**163-7.

23. **Iwamoto, T., K. Mise, A. Takeda, Y. Okinaka, K. Mori, M. Arimoto, T. Okuno, and T. Nakai.** 2005. Characterization of Striped jack nervous necrosis virus subgenomic RNA3 and biological activities of its encoded protein B2. J Gen Virol **86:**2807-16.

24. **Janda, M., and P. Ahlquist.** 1993. RNA-dependent replication, transcription, and persistence of brome mosaic virus RNA replicons in S. cerevisiae. Cell **72:**961-70.

25. **Johnson, K. L., and L. A. Ball.** 1999. Induction and maintenance of autonomous flock house virus RNA1 replication. J Virol **73:**7933-42.

26. **Johnson, K. L., and L. A. Ball.** 1997. Replication of flock house virus RNAs from primary transcripts made in cells by RNA polymerase II. J Virol **71:**3323-7.

27. **Johnson, K. L., B. D. Price, and L. A. Ball.** 2003. Recovery of infectivity from cDNA clones of nodamura virus and identification of small nonstructural proteins. Virology **305:**436-51.

28. **Johnson, K. L., B. D. Price, L. D. Eckerle, and L. A. Ball.** 2004. Nodamura virus nonstructural protein B2 can enhance viral RNA accumulation in both mammalian and insect cells. J Virol **78:**6698-704.

29. **Johnson, K. N., K. L. Johnson, R. Dasgupta, T. Gratsch, and L. A. Ball.** 2001. Comparisons among the larger genome segments of six nodaviruses and their encoded RNA replicases. J Gen Virol **82:**1855-66.

30. **Kaesberg, P., R. Dasgupta, J. Y. Sgro, J. P. Wery, B. H. Selling, M. V. Hosur, and J. E. Johnson.** 1990. Structural homology among four nodaviruses as deduced by sequencing and X-ray crystallography. J Mol Biol **214:**423-35.

31. **Kampmueller, K. M., and D. J. Miller.** 2005. The cellular chaperone heat shock protein 90 facilitates Flock House virus RNA replication in Drosophila cells. J Virol **79:**6827-37.

32. **Kopek, B. G., G. Perkins, D. J. Miller, M. H. Ellisman, and P. Ahlquist.** 2007. Three-dimensional analysis of a viral RNA replication complex reveals a virus-induced mini-organelle. PLoS Biol **5:**e220.

33. **Leeds, P., S. W. Peltz, A. Jacobson, and M. R. Culbertson.** 1991. The product of the yeast UPF1 gene is required for rapid turnover of mRNAs containing a premature translational termination codon. . Genes Dev **5:**2303-2314.

34. **Li, H., W. X. Li, and S. W. Ding.** 2002. Induction and suppression of RNA silencing by an animal virus. Science **296:**1319-21.

35. **Lindenbach, B. D., J. Y. Sgro, and P. Ahlquist.** 2002. Long-distance base pairing in flock house virus RNA1 regulates subgenomic RNA3 synthesis and RNA2 replication. J Virol **76:**3905-19.

36. **Lingel, A., B. Simon, E. Izaurralde, and M. Sattler.** 2005. The structure of the flock house virus B2 protein, a viral suppressor of RNA interference, shows a novel mode of double-stranded RNA recognition. EMBO Rep **6:**1149-55.

37. **Lu, R., M. Maduro, F. Li, H. W. Li, G. Broitman-Maduro, W. X. Li, and S. W. Ding.** 2005. Animal virus replication and RNAi-mediated antiviral silencing in Caenorhabditis elegans. Nature **436:**1040-3.

38. **Miller, D. J., and P. Ahlquist.** 2002. Flock house virus RNA polymerase is a transmembrane protein with amino-terminal sequences sufficient for mitochondrial localization and membrane insertion. J Virol **76:**9856-67.

39. **Miller, D. J., M. D. Schwartz, and P. Ahlquist.** 2001. Flock house virus RNA replicates on outer mitochondrial membranes in Drosophila cells. J Virol **75:**11664-76.

40. **Miller, D. J., M. D. Schwartz, B. T. Dye, and P. Ahlquist.** 2003. Engineered retargeting of viral RNA replication complexes to an alternative intracellular membrane. J Virol **77:**12193-202.

41. **Newman, T. C., M. Ohme-Takagi, C. B. Taylor, and P. J. Green.** 1993. DST sequences, highly conserved among plant SAUR genes, target reporter transcripts for rapid decay in tobacco. . Plant Cell **5:**701–714.

42. **Panavas, T., and P. D. Nagy.** 2003. Yeast as a model host to study replication and recombination of defective interfering RNA of Tomato bushy stunt virus. Virology **314:**315-25.

43. **Perrotta, A. T., and M. D. Been.** 1991. A pseudoknot-like structure required for efficient self-cleavage of hepatitis delta virus RNA. Nature **350:**434-6.

44. **Pogue, G. P., C. C. Huntley, and T. C. Hall.** 1994. Common replication strategies emerging from the study of diverse groups of positive-strand RNA viruses. Arch Virol Suppl **9:**181-94.

45. **Price, B. D., P. Ahlquist, and L. A. Ball.** 2002. DNA-directed expression of an animal virus RNA for replication-dependent colony formation in Saccharomyces cerevisiae. J Virol **76:**1610-6.

46. **Price, B. D., L. D. Eckerle, L. A. Ball, and K. L. Johnson.** 2005. Nodamura virus RNA replication in Saccharomyces cerevisiae: heterologous gene expression allows replication-dependent colony formation. J Virol **79:**495-502.

47. **Price, B. D., M. Roeder, and P. Ahlquist.** 2000. DNA-Directed expression of functional flock house virus RNA1 derivatives in Saccharomyces cerevisiae,

heterologous gene expression, and selective effects on subgenomic mRNA synthesis. J Virol **74:**11724-33.

48. **Price, B. D., R. R. Rueckert, and P. Ahlquist.** 1996. Complete replication of an animal virus and maintenance of expression vectors derived from it in Saccharomyces cerevisiae. Proc Natl Acad Sci U S A **93:**9465-70.

49. **Raghavan, V., P. S. Malik, N. R. Choudhury, and S. K. Mukherjee.** 2004. The DNA-A component of a plant geminivirus (Indian mung bean yellow mosaic virus) replicates in budding yeast cells. J Virol **78:**2405-13.

50. **Reeder, J., and R. Giegerich.** 2004. Design, implementation and evaluation of a practical pseudoknot folding algorithm based on thermodynamics. BMC Bioinformatics **5:**104.

51. **Rivas, E., and S. R. Eddy.** 1999. A dynamic programming algorithm for RNA structure prediction including pseudoknots. J Mol Biol **285:**2053-68.

52. **Sambrook, J. a. R., D.W.** 2001. Molecular cloning: a laboratory manual. Third ed. Cold Spring Harbor Laboratory Press, Cold Spring Harbor, New York.

53. **Scherer, W. F., and H. S. Hurlbut.** 1967. Nodamura virus from Japan: a new and unusual arbovirus resistant to diethyl ether and chloroform. Am J Epidemiol **86:**271-85.

54. **Scherer, W. F., J. E. Verna, and W. Richter.** 1968. Nodamura virus, an ether- and chloroform-resistant arbovirus from Japan: physical and biological properties, with ecologic observations. Am J Trop Med Hyg **17:**120-8.

55. **Selling, B. H., R. F. Allison, and P. Kaesberg.** 1990. Genomic RNA of an insect virus directs synthesis of infectious virions in plants. Proc Natl Acad Sci U S A **87:**434-8.

56. **Sullivan, C. S., and D. Ganem.** 2005. A virus-encoded inhibitor that blocks RNA interference in mammalian cells. J Virol **79:**7371-9.

57. **Taufer, M., M.-Y. Leung, T. Solorio, A. Licon, D. Mireles, R. Araiza, and K. L. Johnson.** 2008. RNAVLab: A virtual laboratory for studying RNA secondary structures based on grid computing technology. Parallel Computing **34:**661-680.

58. **Van Wynsberghe, P. M., and P. Ahlquist.** 2009. 5' cis elements direct nodavirus RNA1 recruitment to mitochondrial sites of replication complex formation. J Virol.

59. **Weeks, S. A., and D. J. Miller.** 2008. The heat shock protein 70 cochaperone YDJ1 is required for efficient membrane-specific flock house virus RNA replication complex assembly and function in Saccharomyces cerevisiae. J Virol **82:**2004-12.

60. **Wu, S. X., P. Ahlquist, and P. Kaesberg.** 1992. Active complete in vitro replication of nodavirus RNA requires glycerophospholipid. Proc Natl Acad Sci U S A **89:**11136-40.

61. **Zhao, K. N., and I. H. Frazer.** 2002. Replication of bovine papillomavirus type 1 (BPV-1) DNA in Saccharomyces cerevisiae following infection with BPV-1 virions. J Virol **76:**3359-64.

62. **Zhong, W., and R. R. Rueckert.** 1993. Flock house virus: down-regulation of subgenomic RNA3 synthesis does not involve coat protein and is targeted to synthesis of its positive strand. J Virol **67:**2716-22.

CURRICULUM VITA

John Rosskopf was born in Honolulu, Hawaii. At a young age, John's family moved to El Paso, Texas where he was raised. He graduated from Burges High School in 1992 and immediately enlisted in the United States Navy. From 1992 to 1998 John served in the navy as a hospital corpsman providing patient care for sailors and marines for routine, and sometimes life-threatening, injuries as well as illnesses. Returning to El Paso, John began his college career at El Paso Community College and subsequently finished his B.S. in Microbiology at the University of Texas at El Paso (UTEP) in the spring of 2006. He was immediately accepted into UTEPs graduate program in Biological Sciences, working in Dr. Kyle Johnson's laboratory. He received his M.S. in Biology in the fall of 2009 and still resides in El Paso with his wife, mother, and three children.

Permanent Address: 4515 Memphis
El Paso, Texas 79903